Surge-type glaciers in the Tien Shan (Central Asia)

Mukherjee, Kriti ; Bolch, Tobias ; Goerlich, Franz ; Kutuzov, S ; Osmonov, A ; Pieczonka, Tino ; Shesterova, Irina

Abstract: Surge-type glaciers have been observed in several mountain ranges of the world. Though Karakoram and Pamir are the hot spots for the occurrence of surge-type glaciers in High Mountain Asia, few surge-type glaciers also exist in Tien Shan. These have not been studied or reported in detail in the recent literature. We have identified 39 surge-type glaciers and five tributary surges in Tien Shan either from available literature or by visual interpretation using available images from the period 1960 until 2014. Out of the 39 glaciers, 9 are confirmed as surge-type, 13 are very probably surge-type, and the remaining are possibly of surge-type. Most of the surge-type glaciers are located in Ak-Shiirak and Central Tien Shan. Compared with the normal glaciers of Tien Shan, the surge-type glaciers are larger, cover higher ranges of elevations, and have shallower slopes. There is no significant difference in aspect. The largest surge events were observed in Central Tien Shan: North Inylchek Glacier (years 1996/1997) and Samoilowich Glacier (years 1992 until 2006) advanced several kilometers. The surge cycle was around 50 years for both of these glaciers. The advance was less pronounced for all other surge-type glaciers during the period ca. 1960–2014. Some of the tributary glaciers behaved differently than the main glaciers in the sense that they continuously advanced during the entire period of our study, whereas the main glaciers have remained stable or retreated.

DOI: https://doi.org/10.1657/AAAR0016-021

Arctic, Antarctic, and Alpine Research, Vol. 49, No. 1, 2017, pp. 147–171
DOI: http://dx.doi.org/10.1657/AAAR0016-021

Surge-type glaciers in the Tien Shan (Central Asia)

K. Mukherjee[1,*], T. Bolch[1,2,*], F. Goerlich[1,2,*], S. Kutuzov[3,*], A. Osmonov[4,*], T. Pieczonka[1,*], and I. Shesterova[5,*]

[1]Institute for Cartography, Technische Universität Dresden, Helmholtzstr. 10, 01069 Dresden, Germany
[2]Department of Geography, University of Zurich, Winterthurer Str. 190, 8057 Zürich, Switzerland
[3]Institute of Geography, Russian Academy of Sciences, Staromonetniy pereulok 29, 119017, Moscow, Russia
[4]Central Asian Institute for Applied Geosciences (CAIAG), Timur Frunze Rd.73/2, 720027 Bishkek, Kyrgyz Republic
[5]Institute of Geography of the Republic of Kazakhstan, Kabanbai Batyr / Pushkin Str. 67/99, 050010 Almaty, Kazakhstan
[*]Authors' email addresses: (K. Mukherjee and T. Bolch are the corresponding authors): mukherjee.kriti@gmail.com, tobias.bolch@geo.uzh.ch, franz.georlich@geo.uzh.ch, s.kutuzov@gmail.com, a.osmonov@caiag.kg, tino.pieczonka@tu-dresden.de, irina_shesterova@mail.ru

A B S T R A C T

Surge-type glaciers have been observed in several mountain ranges of the world. Though Karakoram and Pamir are the hot spots for the occurrence of surge-type glaciers in High Mountain Asia, few surge-type glaciers also exist in Tien Shan. These have not been studied or reported in detail in the recent literature. We have identified 39 surge-type glaciers and five tributary surges in Tien Shan either from available literature or by visual interpretation using available images from the period 1960 until 2014. Out of the 39 glaciers, 9 are confirmed as surge-type, 13 are very probably surge-type, and the remaining are possibly of surge-type. Most of the surge-type glaciers are located in Ak-Shiirak and Central Tien Shan. Compared with the normal glaciers of Tien Shan, the surge-type glaciers are larger, cover higher ranges of elevations, and have shallower slopes. There is no significant difference in aspect. The largest surge events were observed in Central Tien Shan: North Inylchek Glacier (years 1996/1997) and Samoilowich Glacier (years 1992 until 2006) advanced several kilometers. The surge cycle was around 50 years for both of these glaciers. The advance was less pronounced for all other surge-type glaciers during the period ca. 1960–2014. Some of the tributary glaciers behaved differently than the main glaciers in the sense that they continuously advanced during the entire period of our study, whereas the main glaciers have remained stable or retreated.

Introduction

Surge-type glaciers constitute only a small percentage of the world's glaciers and are gathered in clusters, which are nonrandomly distributed over the world (Jiskoot et al., 1998; Sevestre and Benn, 2015). Though small in number, identification, monitoring, and a solid understanding of the causes, mechanisms, and factors influencing glacier surges are crucial, because surging has caused major hazards such as outburst floods of dammed lakes and associated impacts in the proglacial area (Bruce et al., 1987; Jiskoot et al., 1998; Kotlyakov et al., 2008; Häusler et al., 2016). With increased human activity in mountainous areas for various reasons such as habitation, recreation, resource extraction, or transportation, it is important to update our knowledge about the locations of the surging glaciers so that disasters related to hazardous impacts from moving ice can be avoided. Surges can alter the shape of the glacier and change the terrain by erosion of ice with the glacier bed, which may form large boulders and destroy nearby vegetation or man-made infrastructure such as hydroelectric power

stations and villages (Kotlyakov et al., 2008; Kotlyakov, 2004). Monitoring of past surges and assessment of the advance, volume change, and velocities of ice movements during surging may serve as important parameters in predicting the future surges of the same glacier. In addition, these glaciers need special consideration in glacio-hydrological models for assessing past and future impacts of glacier changes on river runoff.

Definitions of surge-type glaciers vary, and their identification is often not straightforward because there is no specific threshold in terms of advance in a certain period of time above which a glacier can be categorized as being surge-type. Glacier surging is a quasiperiodic alternation between long periods (tens to hundreds of years) of slow flow, called quiescent phase or quiescence, and shorter periods of typically 10–1000 times faster flow, called surge phase, active phase, or surge (Dolgoushin and Osipova, 1982; Jiskoot, 2011; Benn and Evans, 2010). The cause of glacier surge has been identified as the relaxation of stresses in the body of the glacier (Dolgoushin and Osipova, 1975). A surge of polythermal glaciers may be initiated due to thickening and steepening in the upper reaches of the glacier, which increases the basal shear stress (Meier and Post, 1969; Murray et al., 2000). When the stress is more than the backward basal drag, the glacier may suddenly advance. For temperate hard-bed glaciers, during surge the high pressure because of the thickening of the glacier changes the basal water conduit system and stops the drainage of water through these channels. This results in increase of water in the glacier bed, which triggers the downward motion and allows the glacier to slide much faster than the normal speed (Kamb, 1987; Barrand and Murray, 2006; Björnsson, 1998). However, in the case of soft-bed glaciers, with increase in thickness of the reservoir, there is a deformation of the sediments in the glacier bed, which promotes the surge further (Murray et al., 2000). Some environmental factors such as extensive ice avalanches and large temperature fluctuations have also been identified as factors causing glacier surge in Karakoram Himalaya (Hewitt, 1969). The cluster of surge glaciers in specific climatic zones also suggests that environmental factors control surging (Post, 1969; Jiskoot et al., 1998.; Sevestre and Benn, 2015). However, it is also true that glacier surges are recurring phenomena caused by some dynamic instability of the glacier system, and they are only indirectly dependent on external factors (Murray et al, 2000; Mayer et al., 2011; Jiskoot et al., 1998; Quincey and Luckman, 2014).

Surge-type glaciers in High Asia are especially common in the Karakoram (Hewitt, 2011; Bolch et al., 2012; Copland et al., 2011; Gardelle et al., 2013; Bhambri et al., 2013; Paul 2015) and the Pamir (Kotlyakov et al., 2008; Osipova and Khromova, 2010; Gardelle et al., 2013, Holzer et al. 2016). Sevestre and Benn (2015) reported a total of 106 and 820 surge-type glaciers in Karakoram and Pamir, respectively. Few surge-type glaciers have also been identified in the Tien Shan (Dolgoushin and Osipova, 1975; Narama et al., 2010; Kotlyakov et al., 2010; Osmonov et al., 2013; Häusler et al., 2016; Pieczonka et al., 2013). However, studies of individual surges in the region are rare, and only recently the volume and elevation changes of Northern Inylchek Glacier, the largest surge-type glacier in Tien Shan, were investigated (Pieczonka and Bolch, 2015; Shangguan et al., 2015).

The available knowledge based on some ground observations as well as satellite image-based studies of Tien Shan glaciers suggest that surge-type glaciers are mostly observed in Central Tien Shan, Ak-Shiirak and Northern Tien Shan (Bondarev, 1961; Bondarev and Zabirov, 1964; Dolgoushin and Osipova, 1975). Dolgoushin and Osipova (1975) mentioned 21 surge-type glaciers in the Tien Shan of which 8 were surging between 1956 and 1970 (Table 1). Sevestre and Benn (2015) identified 11 surge-type glaciers in Tien Shan based on a literature survey.

The reported advances were between 1 and 5 km during 1940–1960 for the glaciers in Central Tien Shan. For example, Mushketov (No. 3 in our numeration in Table 1 and Fig. 1) and Karagul (No. 23) glaciers surged by ~4–5 km in 1956–1957 (Zabirov, 1961; Dyurgerov et al., 1995; Bondarev and Zabirov, 1964; Dolgoushin and Osipova, 1975; Osmonov, 1968). Kaindy Glacier (No. 2) surged in 1960, and its tongue advanced by ~1.3 km compared to its extent in 1943, and both the length and thickness of ice at the tongue significantly increased (Osmonov, 1974). It was reported that the upper left tributary having two branches with northeast and southwest aspects, and its own accumulation zone, served as reservoir for this advance. The tongue of Kaindy Glacier showed high downwasting rates (-1.25 ± 0.49 m yr^{-1}) in the period ca. 1975–1999 despite thick debris cover (Pieczonka and Bolch, 2015), which indicates that during this period the glacier had already shifted to its quiescent phase after the surge. North Inylchek Glacier (No. 1) retreated continuously from 1943 till at least 1990 (Mavlyudov, 1995). Thereafter, it advanced rapidly ~4 km during 1996–1997 (Mavlyudov, 1999; Häusler et al., 2016), experiencing a strong thickening at the tongue during the surge (Pieczonka and Bolch, 2015), and a lowering after 1999 (Shangguan et al., 2015; Häusler et al., 2016). It has been reported in Häusler et al. (2016) that 0.15 km^3 water was displaced by this surge and triggered an outburst flood in the Lower Lake Merzbacher. A recent prominent surge (13% increase in glaciated

TABLE 1

Location and characteristics of identified surge-type glaciers in Tien Shan.

No.	Name	Location	Mountain Range	Length (L) (km)	Area (A) (km^2)	Period of advance	Advance (m)	Area increase (km^2)	Rate of advance (m yr^{-1})	Elevation (m a.s.l.)	Mean Slope (°)	Aspect	Surge Index	References
1	Northern Inylchek	42.23°N, 79.95°E	Central Tien Shan	L_{max} (1997) = 34.38 L_{min} (1992) = 30.72	A_{max} (1997)= 149.5 A_{min} (1995)= 145.4	1990–1991 1995–1997	~1000 3652±45	4.13±0.25	~1625	Z_{max} = 6376 Z_{min} = 3318	24.0	West	1	Mavlyudov, 1995, 1999; Pieczonka and Bolch, 2015; Shangguan et al., 2015
2	Kaindy	42.09°N, 79.70°E	Central Tien Shan	L_{max} (1974) = 25.86 L_{min} (2014) = 24.69	A_{max} (1974)= 90.2 A_{min} (2014)= 88.9	1943–1960 1968–1974	1300 104±13.5	0.03±0.03	~76 ~17	Z_{max} = 5644 Z_{min} = 3222	17.6	West	2	Osmonov, 1974; Dolgoushin and Osipova, 1975; Pieczonka and Bolch, 2015
2a	Tributary to Kaindy	42.06°N, 79.63°E	Central Tien Shan	L_{max} (2014) = 6.74 L_{min} (1974) = 6.05	A_{max} (2014)= 7.38 A_{min} (1974)= 7.15	1974–2014	707±32	0.23±0.06	~17	Z_{max} = 5267 Z_{min} = 3593	21.1	NW	2	This study
3	Mushketov	42.30°N, 79.89°E	Central Tien Shan Adir-tor	L_{max} (1974) = 19.26 L_{min} (2014) = 17.47	A_{max} (1974)= 47.73 A_{min} (2014)= 44.73	ca. 1944–1959 1956–1957	~2460 4300–4500	>4 km^2	~164 ~4400	Z_{max} = 5412 Z_{min} = 3368	17.09	West	1	Bondarev and Zabirov, 1964; Dyurgerov et al., 1995; Dolgoushin and Osipova, 1975
3a	Tributary to Mushketov	42.29°N, 79.96°E	Central Tien Shan	L_{max} (2014) = 5.16 L_{min} (1974) = 4.70	A_{max} (2014)= 4.99 A_{min} (1974)= 4.63	1975–2014	1310±110	0.44±0.06	~35	Z_{max} =5025 Z_{min} = 3629	19.4	NW	2	Osmonov et al., 2013
3b	Tributary to Mushketov	42.28°N, 79.84°E	Central Tien Shan	L_{max} (2014) = 4.93 L_{min} (1974) = 4.43	A_{max} (2014)= 5.01 A_{min} (1974)= 4.55	1977–2014	462±112	0.36±0.07	~12	Z_{max} = 5031 Z_{min} = 3710	22.5	NW	2	Osmonov et al., 2013
3c	Tributary to Mushketov	42.28°N, 79.87°E	Central Tien Shan	L_{max} (2014) = 5.06 L_{min} (1974) = 3.77	A_{max} (2014)= 5.24 A_{min} (1974)= 4.75	1977–2014	505±110	0.49±0.08	~13	Z_{max} = 5047 Z_{min} = 3909	24.8	NW	2	Osmonov et al., 2013
4	Samoilowich	41.00°N, 79.76°E	Central Tien Shan	L_{max} (1960) = 8.87 L_{min} (1992) = 5.78	A_{max} (1960)= 6.94 A_{min} (1992)= 5.43	1992–2006	2687±55	1.22±0.26	~192	Z_{max} = 4995 Z_{min} = 3267	18.2	North	1	Osmonov et al., 2013; Pieczonka and Bolch, 2015
5	Qinbingtan Glacier 74	41.77°N, 79.96°E	Central Tien Shan	L_{max} (1962) = 8.17 L_{min} (2002) = 7.90	A_{max} (1962)= 6.60 A_{min} (2002)= 5.58	2002–2006	34±53.5	0.34±0.16	~9	Z_{max} = 5508 Z_{min} = 3907	13.8	SW	3	Pieczonka et al., 2013; Sevestre and Benn, 2015
6		41.88°N, 80.48°E	Central Tien Shan	L_{max} (2010) = 5.45 L_{min} (1962) = 4.31	A_{max} (2010)= 5.70 A_{min} (1962)= 5.38	1962–2010	1123±55	0.42±0.10	~23	Z_{max} = 4820 Z_{min} = 3454	22.1	NW	2	Pieczonka and Bolch, 2015
7		41.95°N, 80.49°E	Central Tien Shan	L_{max} (1998) = 3.66 L_{min} (1975) = 3.36	A_{max} (2002)= 3.61 A_{min} (1975)= 3.46	1975–1989	276 ±112	0.08±0.11	~20	Z_{max} = 4847 Z_{min} = 3856	22.3	NW	2	Pieczonka and Bolch, 2015
8	Bogatyr	43.03°N, 77.30°E	Northern Tien Shan	L_{max} (1971) = 7.80 L_{min} (1978) = 6.97	A_{max} (1994)= 30.48 A_{min} (1975)= 29.81	1978–1994	405±127	0.60±0.25	~25	Z_{max} = 4523 Z_{min} = 3455	14.0	SE	2	This study
9	South Jangyryk	42.96°N, 77.24°E	Northern Tien Shan	L_{max} (1971) = 6.76 L_{min} (1994) = 5.95	A_{max} (2000)= 8.51 A_{min} (1994)= 7.88	1994–2000	798±62.5	0.62±0.12	~133	Z_{max} = 4549 Z_{min} = 3443	14.9	North	1	This study
10	Zapadniy Aksu (West Ak Suu)	42.85°N, 77.08°E	Northern Tien Shan	L_{max} (1978) = 5.40 L_{min} (2012) = 4.84	A_{max} (1978)= 4.34 A_{min} (2012)= 3.99	1963–1966 1975–1976 1979–1982 1971–1975	 452±115	 0.29±0.11	 ~113	Z_{max} = 4373 Z_{min} = 3467	12.1	North	1	Dyurgerov et al., 1995

TABLE 1
(Continued)

No.	Name	Location	Mountain Range	Length (L) (km)	Area (A) (km^2)	Period of advance	Advance (m)	Area increase (km^2)	Rate of advance (m yr^{-1})	Elevation (m a.s.l.)	Mean Slope (°)	Aspect	Surge Index	References
11	Sarytor-3	41.95° N, 78.27°E	Ak-Shiirak	L_{max} (1980) = 6.02 L_{min} (2013) = 4.44	A_{max} (1973)= 11.17 A_{min} (2013)= 10.07	1964–1980	534±17.5	0.43±0.06	~33	Z_{max} = 4775 Z_{min} = 3752	17.3	NW	2	Pieczonka and Bolch, 2015
12	Davidov	41.85°N, 78.19°E	Ak-Shiirak	L_{max} (1980) = 4.55 L_{min} (1964) = 4.28	A_{max} (1980)= 10.53 A_{min} (1964)= 10.21	1964–1980	280±17.5	0.32±0.05	~18	Z_{max} = 4817 Z_{min} = 3766	15.4	NW	2	This study
13	South Karasai	41.76°N, 78.27°E	Ak-Shiirak	L_{max} (1993) = 4.22 L_{min} (1973) = 3.75	A_{max} (1993)= 5.33 A_{min} (1973)= 4.99	1973–1993	473±60	0.34±0.08	~24	Z_{max} = 4780 Z_{min} = 4063	12.8	South	2	This study
14	South Karasai – S1	41.75°N, 78.26°E	Ak-Shiirak	L_{max} (1964) = 5.19 L_{min} (2011) = 4.57	A_{max} (1964)= 7.72 A_{min} (2011)= 6.70	2011–2013	85±55.5	0.12±0.07	~43	Z_{max} = 4945 Z_{min} = 3823	13.3	West	2	This study
15	South Karasai – S2	41.74°N, 78.25°E	Ak-Shiirak	L_{max} (1980) = 3.86 L_{min} (2014) = 3.50	A_{max} (1980)= 3.15 A_{min} (2014)= 2.96	1964–1980	117±17.5	0.11±0.03	~7	Z_{max} = 4765 Z_{min} = 3868	18.8	North	3	This study
16	Bezymyanny	41.96°N, 78.30°E	Ak-Shiirak	L_{max} (1964) = 5.85 L_{min} (2003) = 4.63	A_{max} (1964)= 5.48 A_{min} (1998)= 4.42	1943–1957 2003–2011	1000 160±62	0.39±0.12	~71 ~12	Z_{max} = 4814 Z_{min} = 3730	18.7	North	2	Dolgoushin and Osipova, 1975; Osmonov et al., 2013
17	Koyandy	41.78°N, 78.33°E	Ak-Shiirak	L_{max} (1973) = 6.03 L_{min} (2013) = 5.10	A_{max} (1973)= 19.72 A_{min} (2013)= 18.66	1964–1973	402±16	0.47±0.06	~45	Z_{max} = 4949 Z_{min} = 3797	15.4	NE	2	Sevestre and Benn, 2015
18	North Karasai	41.79°N, 78.23°E	Ak-Shiirak	L_{max} (1964) = 10.93 L_{min} (2014) = 8.79	A_{max} (1964)= 31.66 A_{min} (2014)= 29.13	1946–1949 1955–1956 1949–1956	~ 1000		~1000	Z_{max} = 4904 Z_{min} = 3783	12.4	SW	1	Bondarev, 1961; Dolgoushin and Osipova, 1975
18a	Tributary to N Karasai 1	41.80°N, 78.21°E	Ak-Shiirak	L_{max} (2014) = 2.78 L_{min} (1973) = 2.64	A_{max} (1993)= 2.31 A_{min} (2014)= 2.22	1973–1993	141±51	0.07±0.036	~7	Z_{max} = 4655 Z_{min} = 3972	18.7	NW	3	This study
19	North Bordu	41.82°N, 78.16°E	Ak-Shiirak	L_{max} (1964) = 5.08 L_{min} (2014) = 4.13	A_{max} (1964)= 5.50 A_{min} (2014)= 4.69	1943–1947 1943–1957	240 260		60 ~19	Z_{max} = 4719 Z_{min} = 3772	16.2	NW	2	Dolgoushin and Osipova, 1975; Bondarev, 1961
20	Chomoi	41.97°N, 78.39°E	Ak-Shiirak	L_{max} (1964) = 4.14 L_{min} (2014) = 3.13	A_{max} (1964)= 5.67 A_{min} (2014)= 5.25	1943–1961	130		~7	Z_{max} = 4890 Z_{min} = 3796	21.6	NE	3	Dolgoushin and Osipova, 1975
21	Besymyanny	42.06°N, 78.66°E	Koiluu Too	L_{max} (1974) =5.31 L_{min} (2014) = 3.32	A_{max} (1973)= 10.28 A_{min} (2014)= 9.02	1956–1957 1964–1974	540 503±16.5	0.09±0.05	540 ~50	Z_{max} = 5156 Z_{min} = 3671	18.2	NE	1	Dolgoushin and Osipova, 1975
22		42.01°N, 78.65°E	Koiluu Too	L_{max} (1964) =5.12 L_{min} (1980) = 4.68	A_{max} (1998)= 6.45 A_{min} (1980)= 6.03	1980–2003	414±58.5	0.39±0.10	~18	Z_{max} = 5017 Z_{min} = 3846	16.3	West	2	Osmonov et al., 2013
23	Karagul	42.27°N, 80.45°E	Central Tien Shan	L_{max} (1975) =32.61 L_{min} (2015) = 32.48	A_{max} (1975)= 168.8 A_{min} (2015)= 168.2	1956–1957	~5000		~5000	Z_{max} = 6264 Z_{min} = 2776	24.3	East	1	Osmonov, 1968
24	Shokalsky	43.08°N, 77.29°E	Northern Tien Shan	L_{max} (1978) =4.27 L_{min} (1994) = 3.30	A_{max} (1972)= 8.25 A_{min} (2014)= 7.46	ca. 1951 (L) 1962–1964 (R) ca. 1968 (L br.) 1994–2000 (R)	No info >300 No info 326±62	0.19±0.08	>150 ~54	Z_{max} = 4471 Z_{min} = 3406	21.5	NW	1	Vilesov and Khonin, 1967; Makarevitch, 1952; Makarevitch and Fedulov, 1974; Cherkasov, 2002
25		42.11°N, 78.58°E	Koiluu Too	L_{max} (2014) = 2.43 L_{min} (1998) = 2.30	A_{max} (2014)= 1.39 A_{min} (1998)= 1.35	1998–2014	131±60	0.034±0.033	~8	Z_{max} = 4663 Z_{min} = 4087	15.3	SW	3	Osmonov et al., 2013

TABLE 1

(Continued)

No.	Name	Location	Mountain Range	Length (L) (km)	Area (A) (km^2)	Period of advance	Advance (m)	Area increase (km^2)	Rate of advance ($m\ yr^{-1}$)	Elevation (m a.s.l.)	Mean Slope (°)	Aspect	Surge Index	References
26	East of Samoilowich	41.99°N, 79.78°E	Central Tien Shan	L_{max} (1960) =8.99 L_{min} (2014) = 7.39	A_{max} (1960)= 10.61 A_{min} (2014)= 10.11	NA	NA	NA		Z_{max} = 5161 Z_{min} = 3620	22.3	NW	3	Pieczonka and Bolch, 2015
27	Ajen Glacier	42.01°N, 80.41°E	Central Tien Shan	L_{max} = 9.14 L_{min} = 9.14	A_{max} = 17.77 A_{min} = 17.77	NA	NA	NA		Z_{max} = 5468 Z_{min} = 3529	19.72	SW	4	Pieczonka et al., 2013
28	Aryansu	41.89°N, 79.80°E	Central Tien Shan	L_{max} = 15.37 L_{min} = 15.37	A_{max} = 32.53 A_{min} = 32.53	NA	NA	NA		Z_{max} = 5420 Z_{min} = 3362	18.44	SE	4	Pieczonka et al., 2013
29		43.09°N, 77.40°E	Northern Tien Shan	L_{max} (1971) = 10.93 L_{min} (2014) = 10.23	A_{max} (1971)= 41.22 A_{min} (2014)= 40.60	NA	NA	NA		Z_{max} = 4929 Z_{min} = 3348	17.42	South	3	This study
30	Jangyryk	42.96°N, 77.20°E	Northern Tien Shan	L_{max} (1971) = 6.61 L_{min} (2014) = 5.27	A_{max} (1971)= 14.85 A_{min} (2014)= 14.24	NA	NA	NA		Z_{max} = 4455 Z_{min} = 3485	15.14	East	3	This study
31	Qong Kozibai	41.94°N, 80.64°E	Central Tien Shan	L_{max} = 20.89 L_{min} = 20.89	A_{max} = 70.11 A_{min} = 70.11	NA	NA	NA		Z_{max} = 6156 Z_{min} = 2800	24.11	South	4	Pieczonka et al., 2013
32		41.05°N, 77.52°E	Southern Tien Shan	L_{max} = 12.28 L_{min} = 12.28	A_{max} = 20.64 A_{min} = 20.64	NA	NA	NA		Z_{max} = 5655 Z_{min} = 3581	19.57	North	3	This study
33		41.05°N, 77.55°E	Southern Tien Shan	L_{max} (1975) = 6.89 L_{min} (2014) = 6.22	A_{max} (1975)= 7.23 A_{min} (2014)= 6.92	NA	NA	NA		Z_{max} = 5147 Z_{min} = 3893	17.14	NW	3	This study
34	Xitalege	41.78°N, 80.20°E	Central Tien Shan	L_{max} = 6.94 L_{min} = 6.94	A_{max} = 9.40 A_{min} = 9.40	NA	NA	NA		Z_{max} = 5030 Z_{min} = 4421	21.36	South	4	Pieczonka et al., 2013
35	Paheluke	41.79°N, 80.24°E	Central Tien Shan	L_{max} = 3.95 L_{min} = 3.95	A_{max} = 4.70 A_{min} = 4.70	NA	NA	NA		Z_{max} = 4811 Z_{min} = 3725	15.78	SE	4	Pieczonka et al., 2013
36	West Qongterang	41.92°N, 80.24°E	Central Tien Shan	L_{max} = 21.97 L_{min} = 21.97	A_{max} = 117.62 A_{min} = 117.62	NA	NA	NA		Z_{max} = 7107 Z_{min} = 3230	25.39	East	4	Pieczonka et al., 2013
37	Unnamed 68	42.26°N, 79.70°E	Central Tien Shan	L_{max} (1974) = 4.13 L_{min} (2002) = 3.80	A_{max} (1974)= 2.70 A_{min} (2002)= 2.58	2002–2006	134±53.5	0.047±0.044	~33	Z_{max} = 4999 Z_{min} = 3627	23.81	NW	2	Sevestre and Benn, 2015
38	East of Besymyanny	42.06°N, 78.72°E	Koiluu Too	L_{max} (1964) = 6.12 L_{min} (2014) = 5.95	A_{max} (1964)= 9.39 A_{min} (2014)= 9.23	NA	NA	NA		Z_{max} = 5162 Z_{min} = 3658	19.09	North	3	This study
39	Petrov	41.90°N, 78.26°E	Ak-Shiirak	L_{max} (1964) = 12.86 L_{min} (2014) = 10.90	A_{max} (1964)= 65.5 A_{min} (2014)= 61.8	NA	NA	NA		Z_{max} = 4893 Z_{min} = 3731	11.26	NW	3	This study

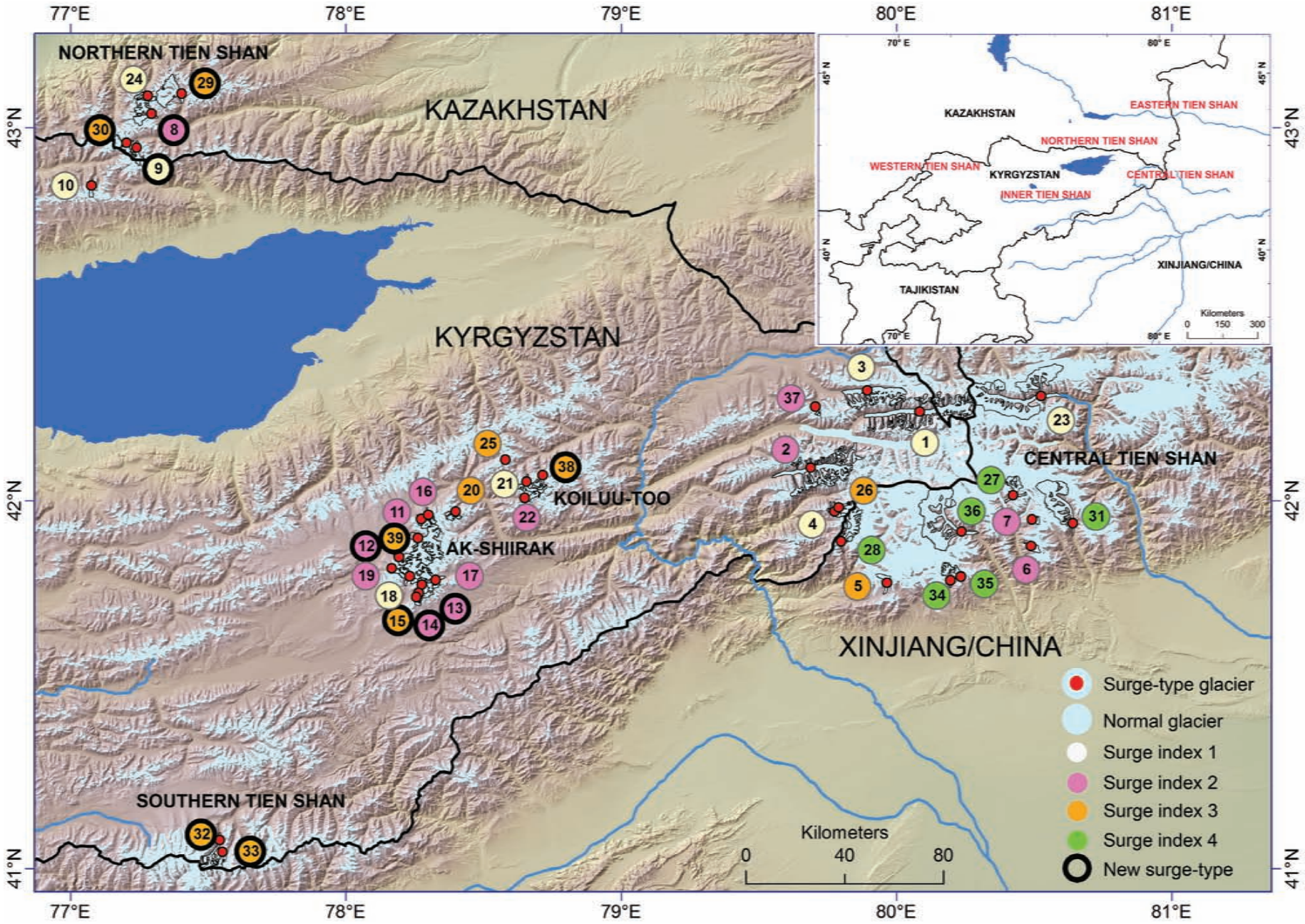

FIGURE 1. Study region and identified surge-type glaciers.

area) was reported for Samoilowich Glacier (No. 4) (Osmonov et al., 2013) during 1990–2010.

Two glaciers of the Ak-Shiirak massif (Bondarev, 1960, 1961, 1963; Bondarev and Zabirov, 1964, Fig. 1) also surged during 1940–1960. The inferred reason for the surge of ~1 km in Northern Karasai Glacier (No. 18) in 1946–1949 and 1955–1956 was not climatic change, but the ice accumulated by the self-growing of the tributaries. Northern Bordu Glacier (No. 19) advanced by 260 m between 1943 and 1957, but overall it retreated by 240 m compared with the terminus in 1932 (Bondarev, 1961).

In Northern Tien Shan, frequent surges were reported for the right and left branches of the Shokalsky Glacier (No. 24) (Dolgoushin and Osipova, 1982). Makarevich (1952) observed a surge in the left branch in 1951, when the ice thickness of the front reached ~60 m. Thereafter both the left and right branches retreated. A stage of surge was again initiated in the upper reaches of the left branch in 1968 which was evident from the increased ice flow velocities (10–20 times). An active advance started in the right branch in 1962, and the thickness in the middle reaches of the right branch of the glacier increased by ~30–40 m until 1964. The tongue of this branch advanced by >300 m and more than 0.027 km^3 ice was involved in this advance. After that the glacier started retreating, and the surface lowered by ~50–55 m until 1967. The surge cycle was estimated to be ~20–24 years for this glacier (Makarevich and Fedulov, 1974; Vilesov and Khonin, 1967; Cherkasov, 2002).

From the above examples, it is evident that there was no common surge period reported in literature. The strongest surges of several kilometers were observed for some of the largest glaciers of the Central Tien Shan. Most of the reported surges are based on some ground observations. Satellite images have also been used to report surges in some other glaciers of this region (Pieczonka et al., 2013; Osmonov et al., 2013; Pieczonka and Bolch, 2015; Häusler et al., 2016), but only North Inylchek Glacier (No. 1) has been studied in more detail recently. Although an extensive investigation of the surge behavior from that region was published in 1975 (Dolgoushin and Osipova, 1975), a more comprehensive and updated assessment is much needed.

The aim of this study is therefore to provide an extensive overview of the current knowledge about surge-type glaciers in the Tien Shan and investigate their characteristics in terms of geographical location (mountain range, latitude, and longitude), length, area, slope, aspect, minimum and maximum elevation, and their changes during surge in terms of length, area, and thickness/volume, with the help of available satellite imagery since the 1960s.

Study Region

The Tien Shan (approximately 40°–45°N, 67°–95°E) is one of the longest mountain ranges in Asia. It stretches from Uzbekistan and southwestern Kyrgyzstan ~2500 km in an east-northeast direction, with the easternmost part located in the Xinjiang Uyghur Autonomous Region of western China (Fig. 1). In the south, Tien Shan links up with the Pamir Mountains and to the northeast meets the Dzhungarian Alatau. The Tien Shan is characterized by a dry and continental climate with the strong seasonal variations that mark most of Central Asia. Temperatures vary with altitude. Aizen et al. (1997) reported a lapse rate of 0.53 °C 100 m^{-1}. Most areas receive strong solar insolation throughout the year with relatively little annual precipitation or cloud cover. Meteorological data indicate that the western and northern peripheries of the Tien Shan have a milder and more temperate climate than the inner regions (Aizen et al., 1995; Solomina et al., 2004). Precipitation in the northwestern (outer) Tien Shan occurs mainly in spring and fall, whereas most of the precipitation takes place in summer in the southeast, central, and inner Tien Shan (Aizen et al., 1996, Aizen et al., 2001, Sorg et al. 2012). Annual precipitation rates decrease from north to south, from over 1000 mm yr^{-1} in the Northern Tien Shan to less than 300 mm yr^{-1} in the Aksai Basin (Koppes et al., 2008). Aizen et al. (1995) reported annual total precipitation increases with altitude up to crest-lines of mountain ranges in all regions of Tien Shan. Over the past four to five decades, the mean annual precipitation has increased in the outer and eastern ranges, but has probably decreased at higher altitudes in the inner ranges (Sorg et al., 2012). The mean annual air temperature (MAAT) at Tien Shan station (41.9°N, 78.2°E, at 3614 m a.s.l., the highest permanent station in the region) is about –7.7 °C, with January being the coldest month and July being the warmest month, having average temperatures of –21.8 °C and 4.3 °C (average of 1960–1997), respectively (Osmonov et al., 2013; Shangguan et al., 2015). MAAT has increased since the 1970s all over the Tien Shan resulting in a prolonged melting season (Aizen et al., 1997; Bolch, 2007; Sorg et al., 2012).

The Tien Shan has more than 6000 glaciers ranging from 2500 m a.s.l. to more than 7000 m a.s.l. (RGI version 4.0; Pfeffer et al., 2014). The total glacierized area is around 16,000 km^2 (Sorg et al., 2012). During the past four decades the overall glacier area and glacier volume of the Tien Shan have significantly reduced (Narama et al., 2010; Sorg et al., 2012; Unger-Shayesteh et al., 2013; Pieczonka and Bolch, 2015). Glacier mass loss in the Tien Shan is reported to be among the highest in the entire High Asia (Gardner et al., 2013; Farinotti et al., 2015) and is strongly related to

temperature increase (Aizen et al., 2006; Bolch, 2007; Koppes et al., 2008; Solomina et al., 2004).

Data and Methods

Data

In order to map the change in terminus position of all known surge-type glaciers and identify new ones of this kind mentioned below, the full Landsat archive was explored, including Multispectral Sensor (MSS), Thematic Mapper (TM), Enhanced Thematic Mapper plus (ETM+), and Operational Land Imager (OLI) data. In addition, we used declassified imagery such as Corona, and Hexagon, one Cartosat-1 stereo pair, Indian Remote Sensing Satellite (IRS) 1C Linear Imaging Self Scanning Sensor (LISS) III data, Satellite Probatoire d'Observation de la Terre 3 (SPOT 3) scenes, and SPOT 5 scenes (Appendix Table A1).

Identification and Assessment of Surge-Type Glaciers

Initially, a list of 27 surge-type glaciers was compiled from existing literature (Table 1). We identified 12 additional surge-type glaciers based on visual image interpretation of morphological features such as presence of looped moraines, and bulging or strongly crevassed tongues (Table 2). In the next step, the terminus changes of all these potential surge-type glaciers have been investigated by using the available images and classified by using the surge index following Sevestre and Benn (2015). We slightly adjusted the index for our study region (Table 2). In order to compare the geometries of surge-type glaciers and the normal glaciers of Tien Shan, typical parameters like length, area, maximum and minimum elevation, elevation range, and slope have been studied. These values were taken from the RGI Vers. 4.0 (Pfeffer et al., 2014; Arendt et al., 2014). The mean (average of all values), median, quartile 1 (Q1), quartile 3 (Q3), minimum and maximum values of each of these parameters have been calculated for both surge-type and normal glaciers. The aspects of surge-type and normal glaciers have been compared using rose diagrams.

Two glaciers that showed the most pronounced surge events, Samoilowich Glacier (No. 4) and North Inylchek Glacier (No. 1), were investigated in more detail in terms of their advance, thickness change during the surge, and the surge frequency. The volume changes for Samoilowich Glacier (No. 4) have been calculated considering a penetration of the Shuttle Radar Topography Mission (SRTM) C-band wave into the snow. The thickness changes for the surge-type glaciers within the Ak-Shiirak mountain range were also studied using the available Digital Terrain Models (DTMs).

Image Coregistration and Glacier Mapping

There were several Corona scenes available for the study area (Table A1). We have generated DTMs from the stereo pairs of 1964 covering the glaciers of Ak-Shiirak massif. All other Corona scenes were coregistered to the master scene (Landsat ETM+, Level 1T) using rubber sheeting (Watson, 1992) available in Erdas Imagine. The rubber sheeting was applied only to a small region surrounding the tongues of the glaciers, and we could achieve coregistration uncertainties of less than one pixel.

TABLE 2

Definitions for surge indexes used in this study.

Surge index	Surge likelihood	Description
1	Confirmed surge-type	Active phase observed with advance of the front with an average advance of >100 m yr^{-1}, presence of geomorphological features related to surge
2	Very probable surge-type	Active phase observed with a lower average advance (between 10 m yr^{-1} and 100 m yr^{-1}), presence of geomorphological features related to surge
3	Possible surge-type A	Slow advance (<10 m yr^{-1}) or evidence of volume gain in the lower ablation region in the past and/or presence of geomorphological features related to surge
4	Possible surge-type B	Neither advance nor clear geomorphological features could be observed, but a surge is mentioned in literature

We used available inventories such as GLIMS (http://www.glims.org) (Raup et al., 2007), RGI version 4.0 (Pfeffer et al., 2014; Arendt et al., 2014), and the outlines by Osmonov et al. (2013) and Pieczonka and Bolch (2015) to extract the polygons of the surge-type glaciers. The glacier outlines were visually checked, and their tongues were manually adjusted according to their extents observed in all images utilized in this study. From these outlines, we then proceeded to estimate the change in length. A glacier profile has been drawn approximately by visual interpretation along the central flow line of each glacier. The length of the profile clipped by the glacier outline corresponding to a particular image has been considered as the length of the glacier in that image. As the glacier outlines were extracted from different images with varying spatial resolutions, it was expected that they would have different levels of accuracies. The uncertainty of estimating length change has been calculated following Hall et al. (2003) as follows:

$$\text{uncertainty} = \sqrt{R_1^2 + R_2^2} + RE, \quad (1)$$

with R_1 and R_2 being the image resolution and RE the registration error.

The precision of glacier mapping is commonly within half a pixel with regard to the glacier perimeter (Paul et al., 2013; Bolch et al., 2010) for clean ice glaciers. However, manual adjustments are needed for debris-covered glaciers. The mapping uncertainties assumed for the different images used in this study are provided in Table A1 (Pieczonka and Bolch, 2015). The uncertainty of the glacier area before and after the surge event was calculated using a buffer around the glacier tongues with the buffer size being the estimated mapping uncertainty mentioned in Table A1 (Bolch et al. 2010). We edited only the changes at the tongues but did not change the upper glacier boundaries; these changes are very minor in comparison to the changes at the tongues of the surge-type glaciers. In addition, several images used were suitable to identify the tongues but not the upper boundaries due to adverse snow conditions.

DTM Generation and Volume Change Estimation

All Hexagon images, some of the Corona stereo pairs, and the Cartosat-1 stereo pair have been used for DTM generation and subsequent orthorectification of the images (Table A1). We made use of several DTMs that were already available, such as those from 1973, 1974, and 1976 KH9 Hexagon data covering large parts of Central and Inner Tien Shan (Pieczonka and Bolch, 2015).

We generated an additional DTM from 1980 based on KH9 Hexagon triplet stereo data (Table A1) for the Ak-Shiirak glaciers. Due to image acquisition on film and long time of film storage, the images had become distorted, and the reseau crosses used to reconstruct the image geometry at the time of acquisition are often shifted from their original locations (Surazakov and Aizen, 2010; Pieczonka et al., 2013; Holzer et al., 2015). Assuming no distortion for the reseau cross at the center of the image, the reference locations of all other crosses were determined and geometrically corrected (cf. Pieczonka et al., 2013). The two registered segments were finally mosaicked in Erdas Imagine, and the mosaicked product was used for subsequent DTM generation using the software ERDAS Photogrammetry 2014. The frame camera model was chosen with a fixed focal length of 0.305 m and flight height of 170 km (Surazakov and Aizen, 2010; Pieczonka et al., 2013). In total, 29 ground control points (GCPs) have been collected from Landsat 7 ETM+ imagery with SRTM3 as vertical reference. These points were located over distinct topographic terrain features like river crossings, mountain ridges, and so forth. In addition, 29 tie points were automatically generated. The resulting root mean square (RMS) error of triangulation was 0.982 pixels. The spatial resolution of the DTM was 30 m.

DTMs from all stereo Corona imagery covering the Ak-Shiirak massif were generated using the Remote Sensing Software Graz (RSG, version 7.46.15, developed by Joanneum Research Graz), using a fixed flying height of 200 km, focal length of 609.6 mm, and other exterior orientation (Table 3). Corona data is available as scanned images in tagged image file (TIF) format with indices from a to d, each having a size of ~85 MB (14 microns scan resolution). The four parts of each image have been merged together in Adobe Photoshop to form the full scene. In the next step, a subset covering the area of interest is extracted from each scene, which has been used subsequently for DTM generation. A Corona adapted image-distortion model is available in RSG, which is essential to set up a geometric model. The number of GCPs collected manually for each subset varied between 27 and 45. Here, we have also used Landsat 7 ETM+ and SRTM as the source to collect horizontal and vertical reference data, respectively. The number of automatically generated tie points varied between 75 and 149. We have achieved RMS errors (for the control points) of less than ~3 pixels in both x and y direction. The spatial resolution of the generated DTMs was 25 m.

In order to investigate the recent surge of Samoilowich Glacier, we used a Cartosat-1 stereo scene (year 2006). The DTM was generated with Toutin's Model in

TABLE 3

Corona camera exterior orientation parameters.

Scene	Omega (ω)	Phi (φ)	Kappa (κ)	Flying height (km)	Focal length (mm)
Forward	0°	15°	61°	200	609.602
Aft		–15°			

ω: viewing angle across flight direction; φ: forward and backward camera tilt; κ: flight direction (0° = east).

Geomatica Ortho Engine 2014 using 17 GCPs and 28 tie points in both stereo images with a RMS_x of 1.84 pixels and a RMS_y of 1.92 pixels. The spatial resolution of the final DTM was 25 m.

All DTMs were coregistered to the SRTM3 master DTM to remove tilts and shifts with respect to the master DTM and for subsequent and reliable glacier thickness change estimation. In a first step, the tilt with respect to the SRTM DTM was minimized by applying a spatial trend correction considering elevation differences over nonglacierized terrain with slopes less than 15° (Bolch et al., 2008; Pieczonka et al., 2013) only. Next, the DTMs were coregistered with respect to the SRTM DTM following Nuth and Kääb (2011). The final displacements between all DTMs and SRTM were less than or equal to one pixel.

The uncertainties of the DTM differences ($E_{\Delta h}$) have been calculated following Gardelle et al. (2013) using Equations (2) to (5), considering elevation bands of 100 m.

$$U_{\Delta h} = \frac{1}{n}\sum_{i=1}^{n} U_{\Delta h(i)} \tag{2}$$

$$\text{Where } U_{\Delta h}(i) = \frac{\sigma_{\Delta h}(i)}{\sqrt{N_e(i)}} \tag{3}$$

$$\text{and, } N_e(i) = \frac{N(i) * P_R}{\sqrt{2 * S}} \tag{4}$$

Here, $U_{\Delta h}$ is the uncertainty of measured elevation difference based on the elevation difference image, $U_{\Delta h}(i)$ is the uncertainty calculated for i'th altitude band, n is the total number of altitude bands, $\sigma_{\Delta h}(i)$ is the standard deviation of the mean elevation change of the nonglacierized terrain in i'th altitude band, $N(i)$ is the total number of pixels in i'th altitude band, P_R is the pixel resolution in meter, and S is the distance (in meters) of spatial autocorrelation of the DTM difference maps.

The penetration (p) of radar waves into firn and snow needs to be considered while using SRTM C band data for DTM differencing and subsequent volume change calculation. We have set this value at 2.2 ± 1.2 m (Pieczonka and Bolch, 2015). The uncertainty in estimating glacier area change has been assumed to be 5% (Paul et al., 2013). Finally, uncertainty of the DTM differencing ($E_{\Delta h}$) has been calculated using Equation (5).

$$E_{\Delta h} = \sqrt{(U_{\Delta h})^2 + (\Delta p)^2 + (\Delta a)^2} \tag{5}$$

Data gaps and mismatching resulting in erroneous elevation values occurred in snow-covered accumulation areas, areas under clouds, or in areas with cast shadows. The resultant outliers in the glacierized terrain were filtered following Pieczonka and Bolch (2015), assuming a nonlinear trend of the variance of elevation differences toward higher elevations by allowing maximum elevation change at the tongues of the glaciers and minimum change at the accumulation regions. All missing pixel values in the accumulation and ablation regions were filled by means of ordinary kriging.

Results

We have found 39 surge-type glaciers of which 12 were newly identified by this study. Out of the five tributary glacier surges, two were additionally identified in this study (Fig. 1, Table 1). Most of these glaciers concentrate in Central Tien Shan and Ak-Shiirak and could be identified as surge-type based on the presence of geomorphological/glaciological features and the rate of advance during the investigated time period (Table 4).

Comparison of Geometries of Surge-Type and Normal Glaciers

The mean values for the length, area, and elevation range of surge-type glaciers are higher and the mean slope is lower compared to the normal glaciers of the Tien Shan (Table 5). Also, the mean of maximum elevation is higher and that of minimum elevation is lower for surge-type glaciers than normal gla-

TABLE 4

Distribution of surge-type glaciers in Tien Shan.

	Number of surge-type glaciers									
	Surge Index 1		Surge Index 2		Surge Index 3		Surge Index 4		Total	
Mountain Range	Main Glacier	Tributary	Main Glacier	Tributary	Main Glacier	Tributary	Main Glacier	Tributary	Main Glacier	Tributary
Central Tien Shan	4	0	4	4 (1*)	2	0	6	0	16	4 (1*)
Ak-Shiirak	1	0	7 (3*)	0	3(2*)	1*	0	0	11 (5*)	1 *
Northern Tien Shan	3 (1*)	0	1*	0	2*	0	0	0	6 (4*)	0
Koiluu Too	1	0	1	0	2(1*)	0	0	0	4 (1*)	0
Southern Tien Shan	0	0	0	0	2*	0	0	0	2 (2*)	0
Total	9 (1*)	0	13 (4*)	4 (1*)	10(7*)	1*	7	0	39 (12*)	5 (2*)

*Bew surge-type glaciers identified from this study.

TABLE 5

Geometric parameters of surge-type and normal glaciers of the Tien Shan.

	Attribute											
	Length (m)		Area (m^2)		Maximum elevation (m)		Minimum elevation (m)		Elevation range (m)		Slope (degree)	
Statistics	S	N	S	N	S	N	S	N	S	N	S	N
Mimimum	1.805	0.035	0.911	0.01	4366	3413	2776	2510	537	8	11.5	2.4
Q1	4.071	0.505	3.814	0.15	4733	4131	3463.5	3689	957	267	15.8	21.6
Median	6.152	0.799	6.151	0.312	4864	4338	3732	3893	1094	407	17.7	26.55
Q3	9.163	1.427	24.263	0.758	5094.5	4575	3888	4084	1500	589	21.3	31.8
Maximum	32.69	62.005	202.658	342.144	7113	7073	4088	5953	3880	4168	28.3	58.6
Mean	8.70	1.23	23.89	1.05	5020.814	4372.946	3668.465	3898.038	1352	475	18.31	26.88

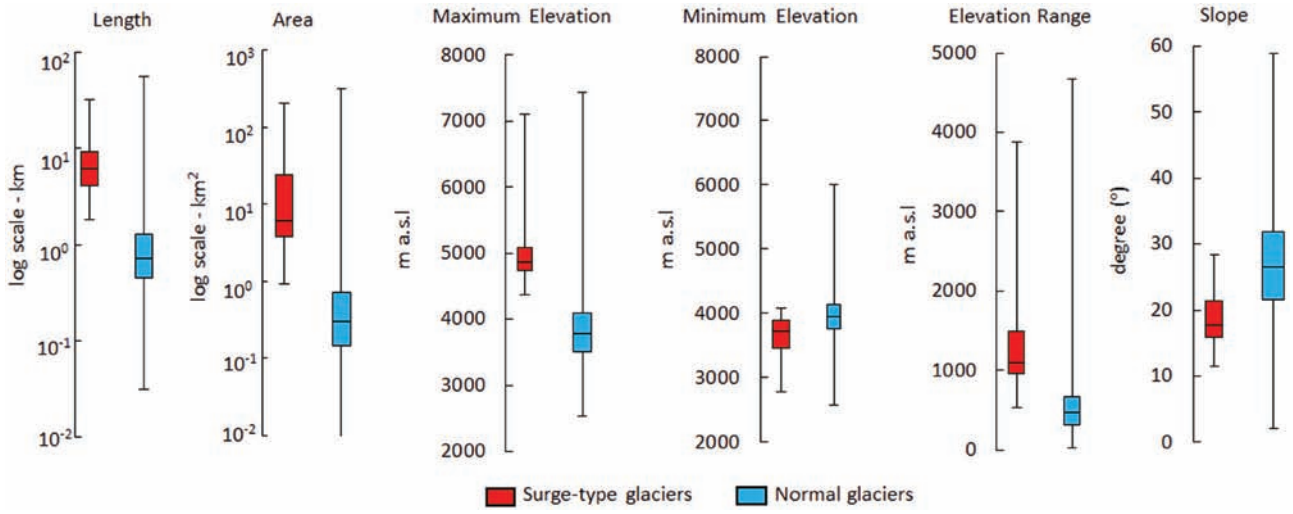

FIGURE 2. Box plots showing the geometries of surge-type and normal glaciers.

ciers (Table 5). Results of a *t*-test yield values of $p \gg 0$ for all parameters except the aspects of surge-type and normal glaciers, which implies that there is a significant difference between the two data sets for all these parameters (see also the box-plots, Fig. 2). Such trends of differences in geometries of surge-type and normal glaciers have been observed all over the world (e.g., Sevestre and Benn, 2015). However, aspect values do not show any significant difference ($p = 0.5$) (Fig. 3). The rose diagrams displaying the frequencies of aspects show that most of the normal as well as surge-type glaciers have north (35.4% and 34.9%, respectively) or northwestern (20.6% and 25.6%, respectively) aspects (Fig. 3).

Relative Length Changes of the Glaciers

The relative length changes of the surge-type glaciers show heterogeneous signals (Fig. 4). North Inylchek Glacier (No. 1) advanced strongly by ~10% (3.7 ± 0.05 km) within a very short period (~2 years). Samoilowich Glacier (No. 4) experienced the most prominent surge as its length increased by ~30% (2.7 ± 0.1 km) from 1992 to 2006. A strong advancement (20%) of glacier No. 6 has been observed from 1998 to 2010 (1.1 ± 0.1 km). The rates of advances were less for other glaciers in the Central Tien Shan (Table 1, Fig. 4).

Among the six surge-type glaciers of Northern Tien Shan, South Jangyryk Glacier (No. 9) and West Ak-Suu Glacier (glacier No. 10) underwent noticeable relative advances. The length increases were ~10% (0.8 ± 0.1 m and 0.5 ± 0.1 m) in 6 years (1994–2000) and 4 years (1971–1975), respectively (Fig. 4). A surge also could be identified for Bogatyr (No. 8) and Shokalsky (No. 24) glaciers (Fig. 4).

Eight of the eleven surge-type glaciers in the Ak-Shiirak range have advanced during our study period, six among them before 2000. However, the rates of advancements were quite low for all the surge-type glaciers in this mountain range compared to other mountain ranges. Some of the glaciers, which were identified from literature as surge-type, such as North Karasai (No. 18), North Bordu (No. 19), and Chomoi (No. 20) Glaciers, have retreated throughout the period of observation. Moreover, Chomoi Glacier separated into two branches in 1993.

We could identify surges at different points of time in three glaciers in the Koiluu Too range, of which Besymyanny Glacier (No. 21) advanced strongly by ~10% between 1964 and 1974 (0.5 ± 0.02 m). Afterward, it has retreated significantly and by 2014 it was reduced to almost 60% of its maximum length. The rates for the other glaciers were slower (Fig. 4).

Samoilowich Glacier

Samoilowich Glacier (No. 4) was in a retreating phase from 1960 to 1992 and in an advancing phase from 1992 to 2006 (Figs. 4, and 5, parts a and b). The maximum length of the glacier was ~8.9 km in 1960. After that it started retreating and reached its minimum length of ~5.8 km in 1992. Thus it retreated by more than 3 km or one-third of its length. After this period of recession, the glacier advanced at an average of 22.5 m yr^{-1} between 1992 and 2000. From 2000 to 2002 the most rapid advance, with an average of 0.8 ± 0.03 km yr^{-1}, was observed. The rate was 0.5 ± 0.03 km yr^{-1} during 2002–2003 and 0.2 ± 0.04 km yr^{-1} during 2003–2006. Altogether, the glacier advanced by 2.7 ± 0.1 km between 1992 and 2006 (Fig. 5, part b,

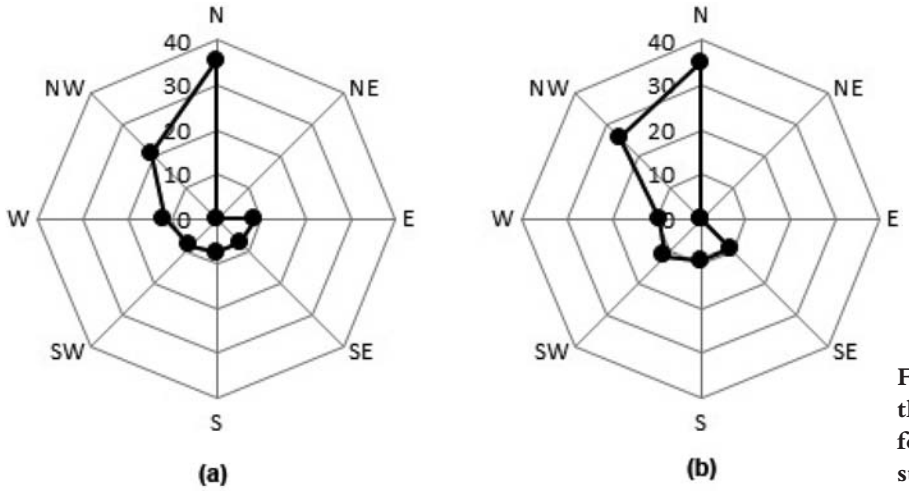

FIGURE 3. Rose diagram showing the frequency of aspect in percentage for (a) normal glaciers, and (b) surge-type glaciers.

and Appendix Fig. A1). Hence, the glacier had an active advancing phase of around 14 (1992–2006) years and experienced a surge cycle of around 50 years (ca. 1960–2006) (Fig. 4). The actual duration of a surge cycle may vary by a few years as the surge phase in any glacier normally starts earlier than any visible advance of the glacier terminus.

The DTM difference revealed that the glacier experienced a clear thickening of as much as 50 ± 5 m in its middle reaches between 1973 and 1999 (Fig. 6, part a). As the ice moved downstream during the surge phase, the glacier strongly thickened at the tongue and lowered in the upper part (Fig. 6, part b). On average, there was a surface lowering of 4 ± 5 m between 1973 and 1999. This loss was a result of a thinning in 70% of the area of the glacier, contributing to a volume loss of 0.056 ± 0.024 km^3 and thickening in the remaining 30% of the area (reservoir area) contributing to a volume gain of 0.033 ± 0.01 km^3.

Differencing the SRTM3 DTM and the Cartosat-1 DTM, which cover the surge phase, revealed a mean thickness change of –2.4 ± 5.6 m, and the volume gain was a little less than the volume loss (volume gain = 0.065 ± 0.01 km^3, volume loss = 0.08 ± 0.02 km^3). Hence, the glacier had probably a slightly negative mass balance during 1999 and 2006. It can be observed in Figure 6, part b, that there was a thickness loss in the middle reaches of the glacier during this period and thickness gain in the lower ablation area as a result of the glacier advance. A thickness increase of maximum 80 ± 5.6 m could be observed in the lower ablation area. The uppermost sections of the glacier remained unaffected. The length and area of the glacier clearly increased as the glacier surged (Fig. 6).

North Inylchek Glacier

North Inylchek Glacier was at its maximum extent in 1943, according to Mavlyudov (1995) (Figs. 4 and 5, part c). Though the same author showed that this glacier advanced slightly between 1990 and 1991, we could not observe this short advance from available satellite images and conclude that the glacier receded continuously from 1967 to 1992 (Fig. 4). From 1992 to 1995, North Inylchek Glacier had a stable front (Figs. 4 and 5, part c). Between 1995 and 1996 it advanced over 0.30 ± 0.02 km (Figs. 5, part d; A1). In 1997 the glacier surface was very crevassed and a fast and pronounced advance of 3.4 ± 0.04 km was observed (Figs. 5, part d; A1). However, the glacier did not extend as far as it had in 1943. From 1997 to 2014 the glacier retreated by 0.3 ± 0.04 km (Fig. 5, part d). Thus, this glacier had a short active phase of around two years (1995–1997) with the most rapid advance in few months only and had a surge cycle of more than 50 years (1943–1997).

The change in thickness of the glacier between ca. 1975 and 1999 could be investigated using KH9 and SRTM DTM. Our results indicate that North Inylchek Glacier experienced a pronounced thickness increase around its tongue (maximum thickness increase of 140 ± 5 m) and a lowering in the middle reaches (Fig. 7; see also Pieczonka and Bolch, 2015; Shangguan et al., 2015). The glacier lost mass at a rate of 0.25 ± 0.1 m w.e. yr^{-1} for the period ca. 1975 until 1999 and experienced a clear lowering of the tongue after 1999, that is, after the surge, with a probably pronounced mass loss of 0.57±0.46 m w.e. yr^{-1} (Shangguan et al., 2015) during 1999–2007.

Glaciers of the Ak-Shiirak Massif

Glaciers in the Ak-Shiirak massif experienced several surges from ca. 1940s to 2014. Overall, we identified 11

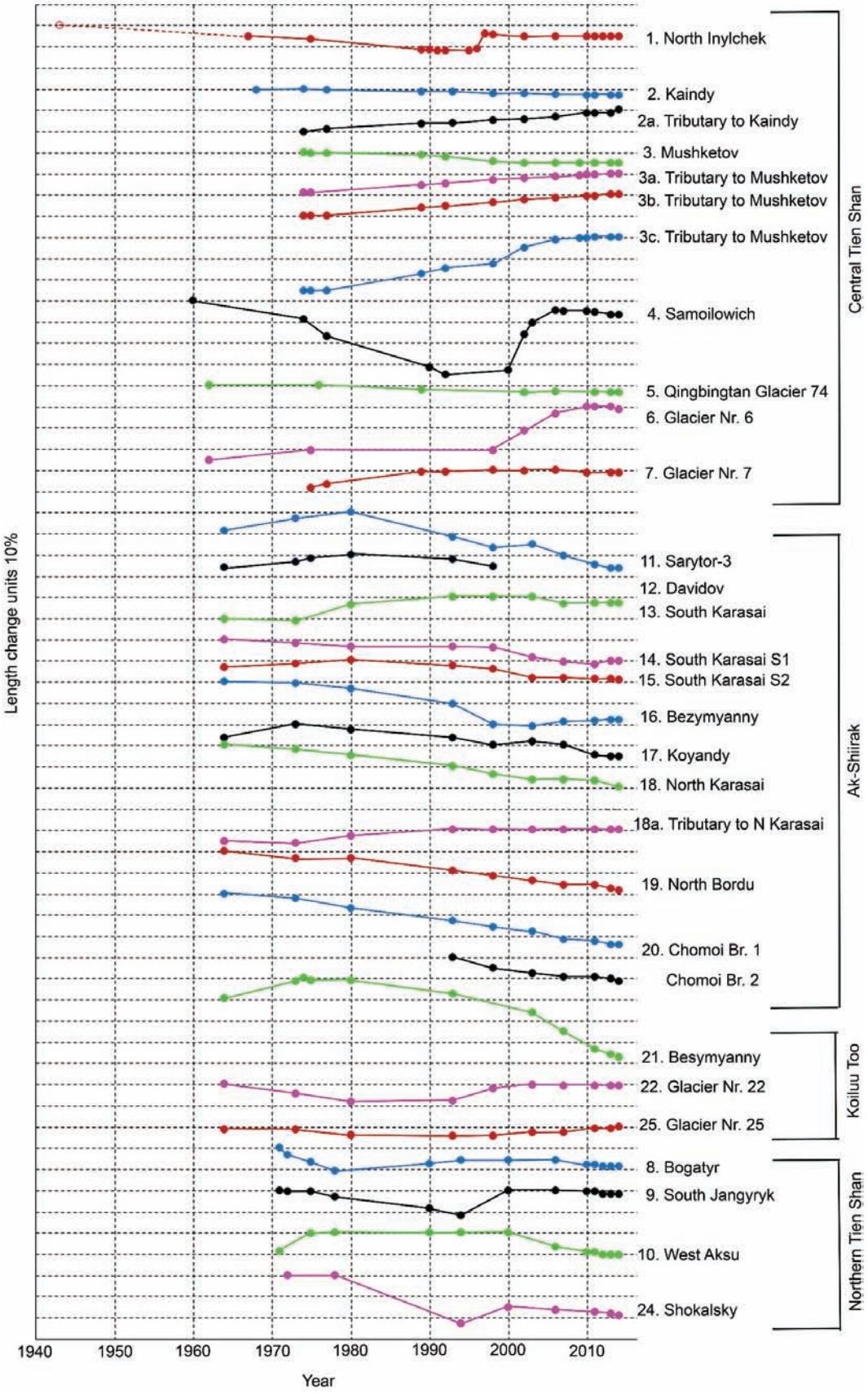

FIGURE 4. Relative length changes of the investigated surge-type glaciers.

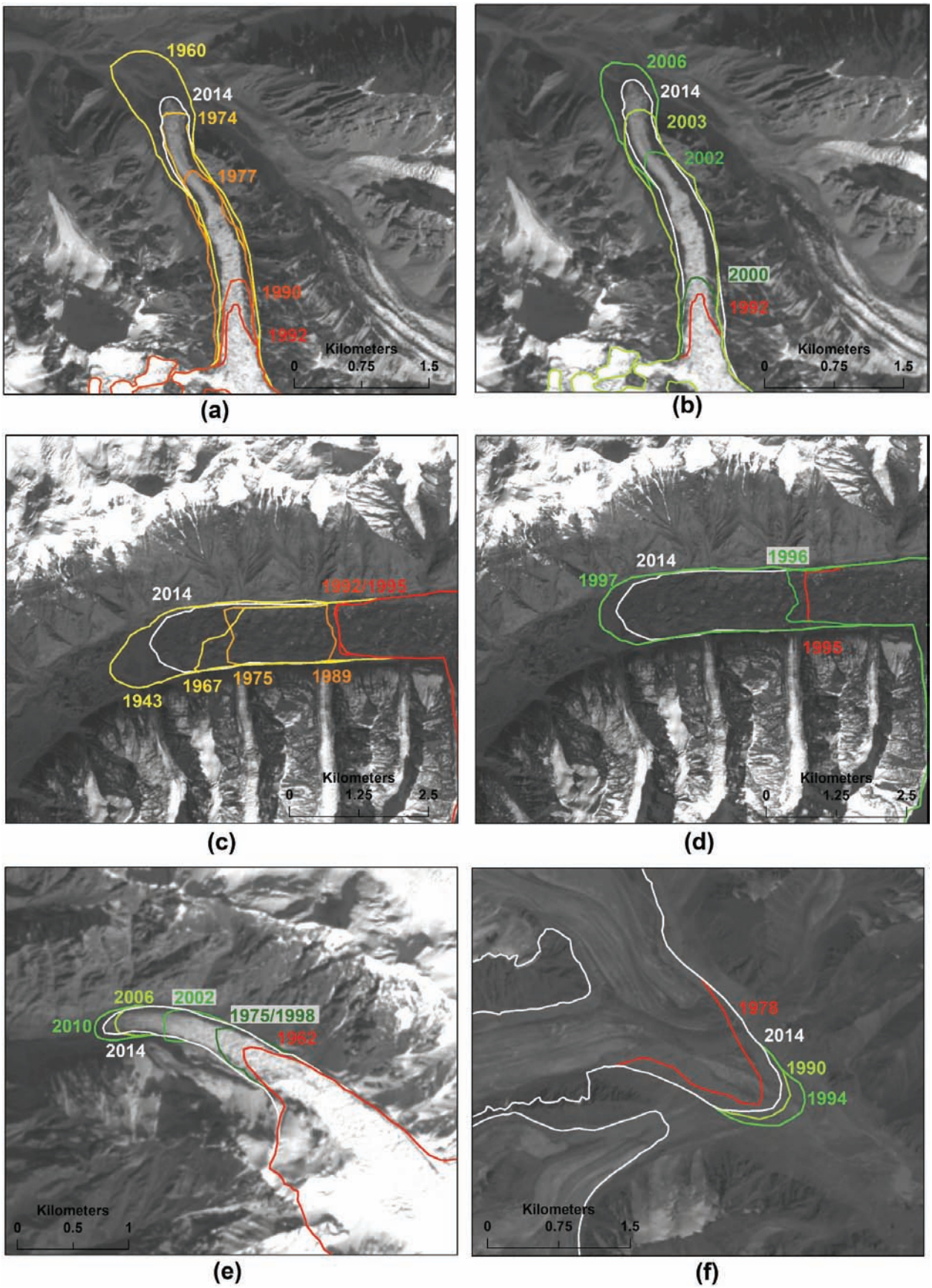

FIGURE 5. Samoilowich Glacier (a) retreat and (b) surge; North Inylchek Glacier (c) retreat and (d) surge; (e) Glacier No. 6 surge; and (f) Bogatyr Glacier (No. 8) surge.

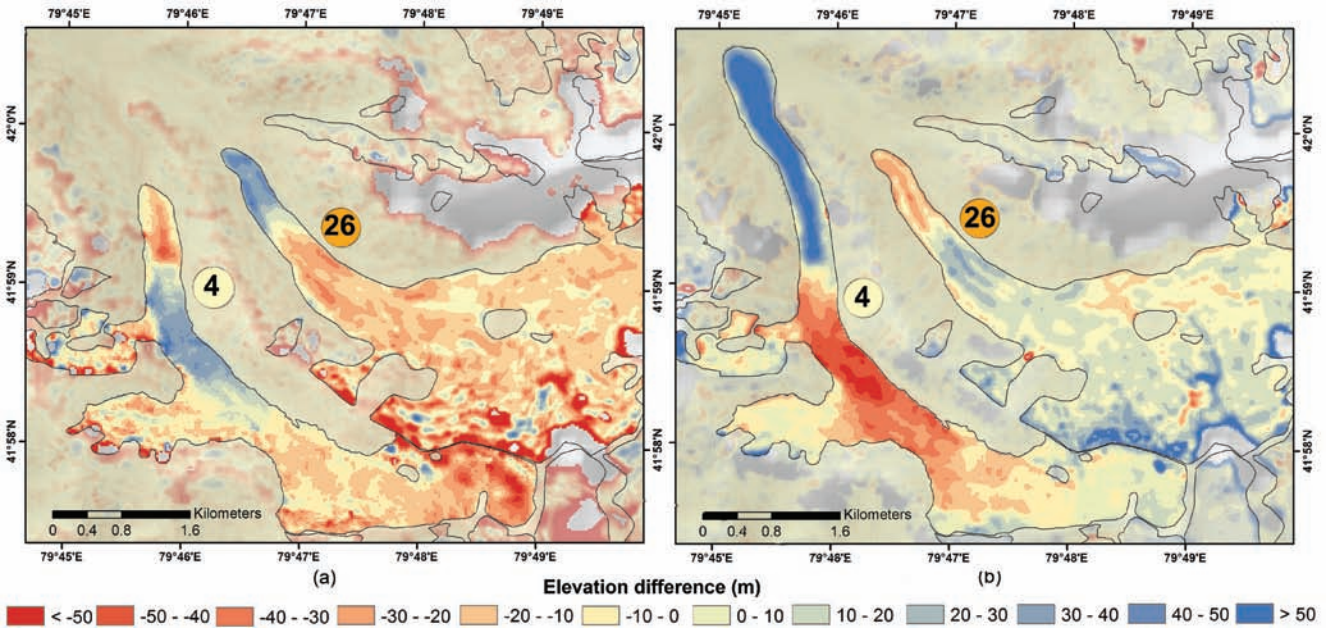

FIGURE 6. Thickness change of Samoilowich Glacier: (a) 1973–1999, and (b) 1999–2006.

surge-type glaciers, of which 5 have not been reported before (Tables 1, 4) but have been identified as surge-type based on geomorphological evidence such as bulging front, crevassed surface, and terminus advance.

The DTM difference of 1973 and 1964 shows that Sarytor-3 (No. 11) and Koyandy (No. 17) glaciers probably experienced a thickening in their lower ablation regions during this period. The terminus of South Karasai Glacier (No. 13) advanced from 1973 to 1993. Davidov Glacier (No. 12) advanced between 1964 and 1980 (Figs. 4, 7, A1), but its tongue was being removed artificially for the construction of a gold mine after 1999 (Jamieson et al., 2015). The tongues of both of these glaciers probably also thickened between 1973 and 1980 while they experienced a thickness lowering in their middle reaches. This indicates that ice has moved from the reservoir area to the receiver area, which resulted in an advance and corresponding thickness gain at the distal parts of the tongues of the glaciers (Fig. 7). However, the thickness increases (Fig. 7) as well as the glacier tongue advances (Fig. 4) are much lower for the surge-type glaciers of Ak-Shiirak than for North Inylchek and Samoilowich glaciers during 1964–2014. All these glaciers have been assigned a surge index 2 (Table 4).

Discussion

Among all the surge-type glaciers identified in this study, 88% are either confirmed, very probable, or possible surge-type glaciers (surge index 1 to 3). For the remaining 12% we could not identify any prominent glaciological or geomorphological feature related to a surge event and therefore state that they are less likely to be surge-type (surge index 4). All the glaciers having surge index 1 or 2 show either rapid, strong advances at different periods, typical indications of surge such as looped moraine, bulging tongue, a strongly crevassed tongue with a steep front, and/or clear lowering in the middle reaches and thickening of the lower reaches of the tongue. The morphological indications are also present in the advancing glaciers that made us, along with the available literature, confident that these glaciers should be classified as surge-type. Glaciers for which advances were very slow or not present during the period of our study, but in which we could identify one of the geomorphological/glaciological features, were classified as possible surge-type glaciers. We think that for these glaciers surges might have smaller active phases or are of small magnitude, and might have remained unnoticed using our approach because of uneven temporal gaps and/or insufficient spatial and temporal resolutions of the satellite images used in this study (Herreid and Truffer, 2015; Willis, 1995). It might also well be possible that further surge-type glaciers in the vast Tien Shan exist, which we missed. This could especially be true for smaller glaciers, for which surges are more difficult to identify as the smaller relative length changes may not be resolved spatially and/or temporally by the available satellite images. The geomorphological/glaciological features are also more difficult to detect in smaller glaciers from visual in-

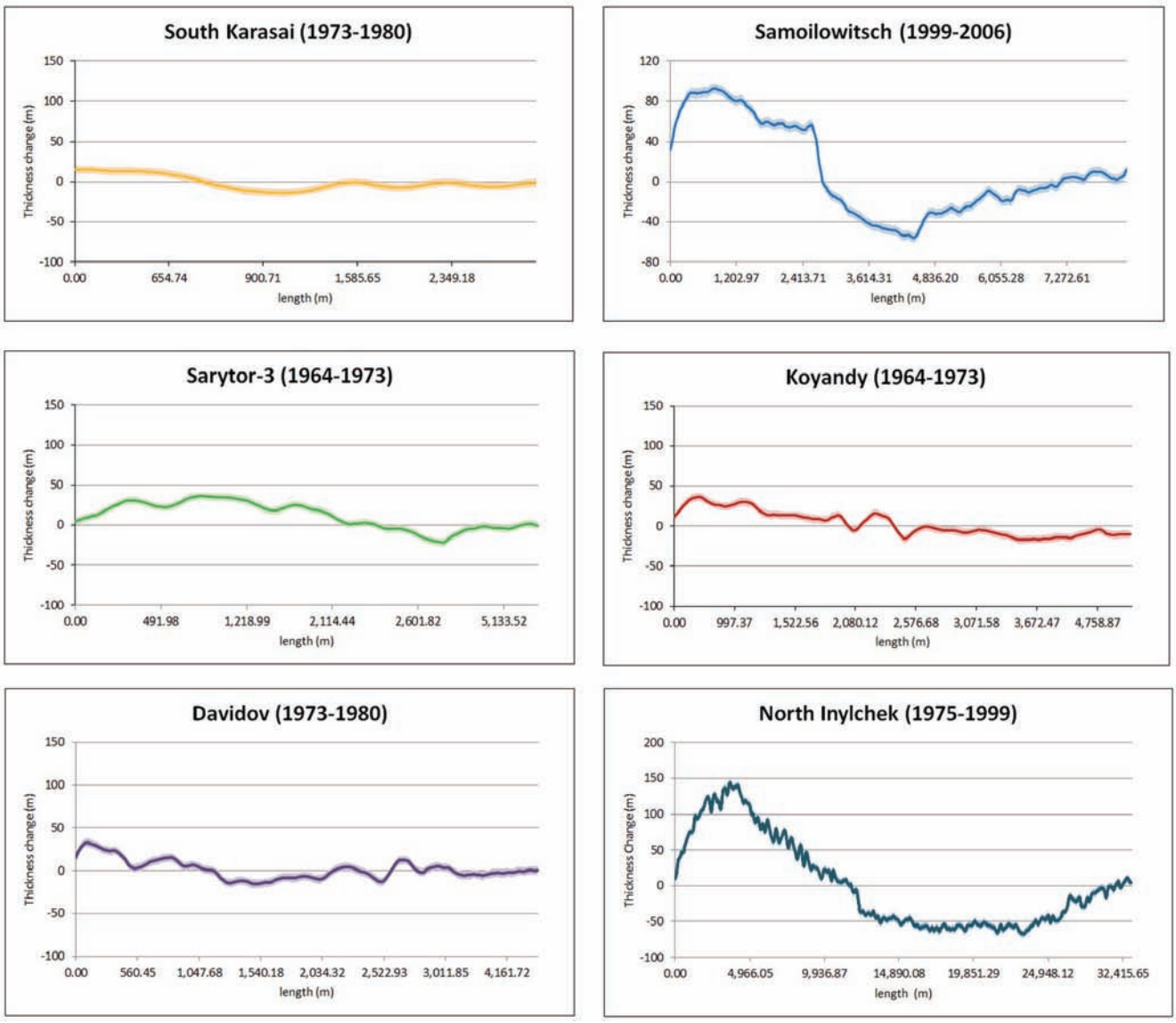

FIGURE 7. Thickness change along glacier profile based on the available bi-temporal Digital Terrain Models (DTMs), which include the surge period for each of the selected glaciers.

terpretation using satellite images only (Hamilton and Dowdeswell, 1996).

It is also possible that a glacier may gain thickness, but does not advance or only slightly advances, which is evident for some of the glaciers for which a thickness gain was observed in earlier studies (e.g., Nos. 26, 27, 28, 31, 34, 35, 36; Fig. 4), but no significant advance could be noticed in the present study. All these glaciers are located in Central Tien Shan, where most of the surges have been reported. Length change (advance or retreat) is not always the best indicator for identifying a surge-type glacier. For example, it can be observed in Figure 8 that the overall length at the central flowline of Bogatyr Glacier (No. 8), which surged during 1978–1994 (Table 1, Fig. 4), has remained almost constant even long after the surge, that is, until 2008. However, the thickness has reduced considerably by 2008 compared to the thickness in 1985. Similarly, Kaindy Glacier (No. 2) also experienced high downwasting rates after its surge in 1960, but its length has not changed much (Fig. 4). The surface dynamics often provide important information on surging, as a glacier moves 10–1000 times faster during its surge phase. Therefore, a combined study including length change, thickness change, and velocity is needed to draw a firm conclusion. We studied mainly length change for all the identified surge-type glaciers, and classified the surge-type glaciers based on that information in addition to morphometric indicators.

We also found some tributary surges, which advanced into the main trunk. Tributary surges have also

been observed in other mountain ranges in High Asia such as the Karakoram (Hewitt, 2007; Paul, 2015; Belò et al., 2008). However, these surges are even more difficult to detect, since there is often no clear boundary between the tributary and the main glacier trunk. We only selected those for which we could identify clear evidence of advance.

The length and area of a glacier and glacier surface slope have been shown to have an effect on glacier surge mechanisms (Clarke, 1991; Jiskoot et al., 2000). The greater length and lesser surface slope increases the subglacial water pressure and results in enhanced basal sliding during surge. Longer glaciers with shallower slopes also have a higher probability of becoming thicker and storing more water (Lingle and Fatland, 2003), and they have a higher chance of eroding the bed of the glaciers (Jiskoot et al., 2000), which are also responsible for surging. It was found in our analysis that surge-type glaciers of Tien Shan are also longer and bigger in area, cover a higher range of elevation, and have shallower slopes than the normal glaciers of Tien Shan—like the surge-type glaciers in the other parts of the world (Sevestre and Benn, 2015; Grant et al., 2009; Jiskoot et al., 2000; Barrand and Murray, 2006).

Sixteen out of the thirty-nine surge-type glaciers are in Central Tien Shan, where the highest two peaks (reaching 7000 m a.s.l. or above) are located. A further hot spot of surges is the Ak-Shiirak massif (highest elevation above 5000 m a.s.l.), where 11 surge-type glaciers have been identified; however, the surges were much less prominent there during our period of observation (1964–2014).

The active phases for some of the largest surge-type glaciers of Tien Shan, such as North Inylchek (No. 1), Mushketov (No. 3), North Karasai (No. 18), and Karagul (No. 23) Glaciers have been observed to be ~1–2 years, and the advance varied between ~1 and 5 km (Table 1, Fig. 1). Surge-type glaciers having longer active phases are smaller in size, e.g., 14 years for Samoilowich (No. 4) Glacier, 16 years for Bogatyr (No. 8) glacier, 14 years for Bezymyanny (No. 16) Glacier etc. (Table 1). Active phases of up to 15 years were also described for surge-type glaciers in Svalbard (Dowdeswell et al., 1991; Jiskoot, 2011), up to 12 years for Pamir (Kotlyakov et al., 2008), and >15 years for some of the Karakoram glaciers (Paul, 2015).

For the two glaciers with the most prominent surge we could identify a more or less full surge cycle. The length of the surge cycle is around 50 years for both glaciers. The right branch of Shokalsky Glacier (No. 24) has been reported to have surged in 1962–1964 (Vilesov and Khonin, 1967; Makarevich and Fedulov, 1974) and it again surged in 1994–2000 as observed in this study. Thus it can be inferred that the surge cycle for this glacier is ~30 years. As we could not identify repeated surges for other glaciers, we conclude that the quiescent phase is relatively long for all surge-type glaciers in the Tien Shan, and surge is not so frequent as, for example, for some of the surge-type glaciers in the Karakoram (Paul, 2015; Quincey et al., 2015, Quincey and Luckman, 2014).

Available geodetic studies suggest that glaciers in the surging phase do not significantly change their overall

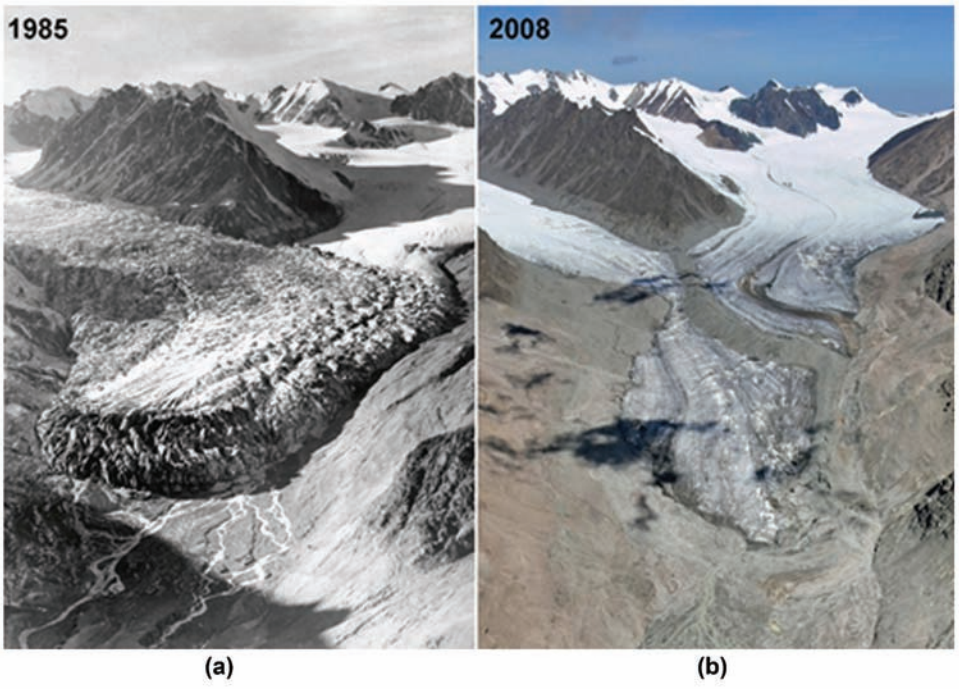

FIGURE 8. Bogatyr Glacier: (a) during the surge phase in 1985 (Institute of Geography, Almaty), and (b) after the surge in 2008 (V. Blagoveshchenskiy).

volume much, can be both slightly negative and positive, and usually the signal is smaller than the uncertainty (Gardelle et al., 2013; Pieczonka and Bolch, 2015). This is in line with our findings for Samoilowich (No. 4) Glacier, which revealed that overall the glacier was in balance or showed a slightly negative mass budget during surge (1999–2006). During the surge event a significant amount of ice is translocated to lower elevations and is there, hence, prone to melt and even thick debris cover cannot prevent the ice from melting. This effect can be clearly identified for the debris-covered North Inylchek (No. 1) and Kaindy (No. 2) glaciers in Central Tien Shan (Pieczonka and Bolch, 2015, Shangguan et al. 2015).

Climatic Considerations

The mean annual air temperature in the Tien Shan increased during the past several decades, but the precipitation did not change significantly (Aizen et al., 1997; Osmonov et al., 2013; Bolch, 2007). As a result, most of the Tien Shan glaciers retreated and, on average, lost mass during that time period (Narama et al., 2010; Kutuzov and Shahgedanova, 2009; Sorg et al., 2012; Pieczonka and Bolch, 2015; Farinotti et al., 2015). There was no fixed time of surging, and different glaciers surged in different years. Therefore, there was no clear trend of glacier surging that could be related to the climatic variation during those past decades. This also implies that although there is a high chance of occurrence of surge-type glacier clusters in specific climatic zones as shown by Sevestre and Benn (2015), the surge event itself is triggered by internal glaciological factors. However, increased temperature during the last decades may have some influence on the strength of glacier surging as we observed that both North Inylchek (No. 1) and Samoilowich (No. 4) glaciers, which surged most, did not advance as much as their earlier maximum extents. Also, some of the Ak-Shiirak glaciers, which had been reported as surge-type in available literature, have retreated considerably throughout.

Conclusions

We have used a variety of high- to medium-resolution satellite images of different dates from the 1960s to 2014 to record surge events in Tien Shan glaciers. We found 39 glaciers and 5 tributary glaciers that showed characteristics related to surges. The surge activity could be confirmed or is very probable for 22 of these 39 glaciers. Most of the surge-type glaciers are located in Central Tien Shan and Ak-Shiirak, which have the highest mountain peaks and colder and drier climate than the outer regions. The most pronounced absolute advance was observed for North Inylchek Glacier, which is the longest among all surge-type glaciers identified in this study. However, the most pronounced relative advance was observed for Samoilowich Glacier, which is much shorter. All the tributary glaciers identified as surge-type have continuously advanced throughout our study period. The rate of advance was more pronounced for some of the glaciers from Central and Northern Tien Shan, and more gradual for the glaciers of Ak-Shiirak. We could identify the surge cycle to be ~30–50 years for three of the glaciers. For the other glaciers we could not identify repeated surge events. Hence, we conclude that the quiescent phase is comparatively long for the surge-type glaciers of Tien Shan and not as heterogeneous as, for example, in the Karakoram, where both short and long active phases as well as quiescent phases have been observed. No clear connection of climatic effects on glacier surge could be found. However, a decrease in maximum extents of the glaciers during surge and retreat of most of the surge-type glaciers during past one/two decades may indicate a reduction in surging tendency in this region.

Author Contributions

T. Bolch designed the study and guided the analysis. K. Mukherjee generated the 1980 Hexagon DTM for Ak-Shiirak, performed all analysis, and wrote the draft of the manuscript. T. Pieczonka generated the Cartosat-1 DEM and the Hexagon DEM for Central Tien Shan. F. Goerlich generated the Corona DTMs. S. Kutuzov, I. Shesterova, and A. Osmonov compiled the information from the Soviet literature. All authors contributed to the final form of the manuscript.

Acknowledgments

This work was conducted within the framework of the projects "Water Resources in the Aksu-Tarim-River Catchment of Western China and the Effects of Climate Change (AKSU-TARIM) supported by the Deutsche Forschungsgemeinschaft (DFG, Code BO 3199/2-1) and the project Sustainable Management of River Oases along the Tarim River/China (SuMaRiO) funded by BMBF (Code 01 LL 0918 B). We thank V. Kotlyakov (Russian Academy of Sciences) and I. Severskiy (Institut of Geography, Almaty) for the comments and the general support. We are also thankful to the anonymous reviewers whose comments have significantly improved the overall structure and contents of the manuscript.

References Cited

Aizen, E. M., Aizen, V. B., Melack, J. M., Nakamura, T., And Ohta, T., 2001: Precipitation and atmospheric circulation patterns at mid-latitudes of Asia. *International Journal of Climatology,* 21: 535–556.

Aizen, V. B., Aizen, E. M., and Melack, J. M., 1995: Climate, snow cover, glaciers and runoff in the Tien Shan, Central Asia. *Journal of the American Water Resources Association*, 31(6): 1113–1129.

Aizen, V. B., Aizen, E. M., and Melack, J. M., 1996: Precipitation, melt and runoff in the northern Tien Shan. *Journal of Hydrology,* 186: 229–251.

Aizen, V. B., Aizen, E. M., Melack, J. M., and Dozier, J., 1997: Climatic and hydrologic changes in the Tien Shan, Central Asia. *Journal of Climate*, 10(6): 1393–1404.

Aizen, V. B., Kuzmichenok, V. A., Sorazakov, A. B., and Aizen, E. M., 2006: Glacier changes in the central and northern Tien Shan during the last 140 years based on surface and remote-sensing data. *Annals of Glaciology,* 43: 202–213.

Arendt, A. A., Bliss, A., Bolch, T., Cogley, J. G., Gardner, A., Hagen, J. O., Hock, R., Huss, M., Kaser, G., Kienholz, C., Pfeffer, W. T., Moholdt, G., Paul, F., Radić, V., Andreassen, L., Bajracharya, S., Barrand, N., Beedle, M., Berthier, E., Bhambri, R., Brown, I., Burgess, E., Burgess, D., Cawkwell, F., Chinn, T., Copland, L., Gurney, S., Hagg, W., Hall, D., Haritashya, U. K., Hartmann, G., Helm, C., Herreid, S., Howat, I., Kapustin, G., Khromova, T., König, M., Kohler, J., Kriegel, D., Kutuzov, S., Lavrentiev, I., Le Bris, R., Lund, J., Manley, W., Mayer, C., Miles, E., Li, X., Menounos, B., Mercer, A., Mölg, N., Mool, P., Nosenko, G., Negrete, A., Nuth, C., Pettersson, R., Racoviteanu, A., Ranzi, R., Rastner, P., Rau, F., Raup, B., Rich, J., Rott, H., Schneider, C., Seliverstov, Y., Sharp, M., Sigurðsson, O., Stokes, C., Wheate, R., Winsvold, S., Wolken, G., Wyatt, F., and Zheltyhina, N., 2014: *Randolph Glacier Inventory—A Dataset of Global Glacier Outlines: Version 4.0*. Boulder, Colorado: National Snow and Ice Data Center, GLIMS Technical Report, Digital Media.

Barrand, N. E., and Murray, T., 2006: Multivariate controls on the incidence of glacier surging in the Karakoram Himalaya. *Arctic, Antarctic, and Alpine Research,* 38(4): 489–498.

Belò, M., Mayer, C., Smiraglia, C., and Tamburini, A., 2008: The recent evolution of Liligo glacier, Karakoram, Pakistan, and its present quiescent phase. *Annals of Glaciology*, 48: 171–176.

Benn, D., and Evans, D. J. A., 2010: *Glaciers and Glaciation*. 2nd edition. London: Routledge, 816 pp.

Bhambri, R., Bolch, T., Kawishwar, P., Dobhal, D. P., Srivastava, D., and Pratap, B., 2013: Heterogeneity in glacier response in the upper Shyok valley, northeast Karakoram. *The Cryosphere*, 7: 1385–1398.

Björnsson, H., 1998: Hydrological characteristics of the drainage system beneath a surging glacier. *Nature,* 395: 771–774.

Bolch, T., 2007: Climate change and glacier retreat in northern Tien Shan Kazakhstan/Kyrgyzstan) using remote sensing data. *Global and Planetary Change*, 56: 1–12.

Bolch, T., Buchroithner, M. F., Pieczonka, T. and Kunert, A., 2008: Planimetric and volumetric glacier changes in Khumbu Himalaya since 1962 using Corona, Landsat TM and ASTER data. *Journal of Glaciology*, 54: 592–600.

Bolch, T., Menounos, B., and Wheate, R., 2010: Landsat-based inventory of glaciers in western Canada. *Remote Sensing of Environment,* 114: 127–137.

Bolch, T., Kulkarni, A., Kääb, A., Huggel, C., Paul, F., Cogley, J. G., Frey, H., Kargel, J. S., Fujita, K., Scheel, M., Bajracharya, S., and Stoffel, M., 2012: The state and fate of Himalayan glaciers. *Science,* 336(6079): 310–314.

Bondarev, L. G., 1960: Nedavnee nastupanie odnogo iz krupneishyh lednikov Tian Shania (Recent advance of one of the largest glaciers in Tien Shan). *Data of Glaciological Studies in Tien Shan,* 2: 21–26 (in Russian).

Bondarev, L. G., 1961: Evolution of some Tien Shan glaciers during the last quarter of the century. *IAHS Publication,* 54: 412–419.

Bondarev, L. G., 1963: Ocherki po oledeneniu massiva Ak-Shyirak (Studies of Ak-Shiirak massif glaciation). Frunze: Kyrgyz SSR Academy of Sciences Publication, 202 pp. (in Russian).

Bondarev, L. G., and Zabirov, R. D., 1964: Kolebanie lednikov bnutrennego Tian Shania v poslednie desiatiletia (Fluctuations of glaciers in inner Tien Shan over recent decades). *Data of Glaciological Studies,* 9: 125–130 (in Russian).

Bruce, R. H., Cabrera, G. A., Leiva, J. C., and Lenzano, L. E., 1987: Correspondence. The 1985 surge and ice dam of Glacier Grande del Nevado del Plomo, Argentina. *Journal of Glaciology,* 33(113): 131–132.

Cherkasov, P. A., 2002: Sovremennoe sostoyanie lednikov Ili-Balkhashskogo regiona (Present state of glaciers in Ili-Balkhash region). *Sovremennoe sostoyanie basseyna ozera Balkhash.: Almaty*, 141–198 (in Russian).

Clarke, G. K. C., 1991: Length, width and slope influences on glacier surging. *Journal of Glaciology*, 37(126): 236–246.

Copland, L., Sylvestre, T., Bishop, M. P., Shroder, J. F., Seong, Y. B., Owen, L. A., Bush, A., and Kamp, U., 2011: Expanded and recently increased glacier surging in the Karakoram. *Arctic, Antarctic, and Alpine Research,* 43: 503–516.

Dolgoushin, L., and Osipova, G., 1975: Glacier surges and the problem of their forecasting, *IAHS Publication,* 104: 292–304.

Dolgoushin, L. D., and Osipova, G. B., 1982: Pulsiruushie ledniki (Surging glaciers). *Leningrad: Gidrometeoizdat Publication*, 192 pp. (in Russian).

Dowdeswell, J. A., Hamilton, G. S., and Hagen, J. H., 1991: The duration of the active phase on surge-type glaciers: contrasts between Svalbard and other regions. *Journal of Glaciology,* 37(127): 388–400.

Dyurgerov, M. B., Liu, C., and Xie, Z., 1995: Oledenenie Tian Shania (Tien Shan glaciation). Moscow: *VINITI,* 237 pp. (in Russian).

Farinotti, D., Longuevergne, L., Moholdt, G., Duethmann, D., Mölg, T., Bolch, T., Vorogushyn, S., and Guentner, A., 2015: Substantial glacier mass loss in the Tien Shan over the past 50 years. *Nature Geoscience,* 8: 716–722.

Gardelle, J., Berthier, E., Arnaud, Y., and Kääb, A., 2013: Region-wide glacier mass balances over the Pamir-Karakoram-Himalaya during 1999–2011. *The Cryosphere,* 7(6): 1263–1286.

Gardner, A. S., Moholdt, G., Cogley, J. G., Wouters, B., Arendt, A. A., Wahr, J., Berthier, E., Hock, R., Pfeffer, W. T., Kaser, G., Ligtenberg, S. R. M., Bolch, T., Sharp, M. J., Hagen, J. O., Broeke, M. R., and Paul, F., 2013: A reconciled estimate of glacier contributions to sea level rise: 2003–2009. *Science,* 340(6134): 852–857.

Grant, K. L., Stokes, C. R., and Evans, S., 2009: Identification and characteristics of surge-type glaciers on Novaya Zemlya, Russian Arctic. *Journal of Glaciology*, 55(194): 960–972.

Hall, D. K., Bahr, K. J., Shoener, W., Bindschadler, R. A., and Chien, J. Y. L., 2003: Consideration of the errors inherent in mapping historical glacier positions in Austria from the ground and space. *Remote Sensing of Environment,* 86(4): 566–577.

Hamilton, G. S., and Dowdeswell, J. A., 1996: Controls on glacier surging in Svalbard. *Journal of Glaciology,* 42(140): 157–168.

Häusler, H., Ng, F., Kopency, A., and Leber, D., 2016: Remote-sensing-based analysis of the 1996 surge of Northern Inylchek Glacier, central Tien Shan, Kyrgyzstan. *Geomorphology*, 273: 292–307.

Herreid, S., and Truffer, M., 2015: Automated detection of unstable glacier flow and a spectrum of speedup behavior in the Alaska Range. *Journal of Geophysical Research: Earth Surface,* 121(1): 64–81.

Hewitt, K., 1969: Glacier surges in the Karakoram Himalaya (Central Asia), *Canadian Journal of Earth Sciences,* 6: 1009–1018.

Hewitt, K., 2007: Tributary glacier surges: an exceptional concentration at Panmah Glacier, Karakoram Himalaya. *Journal of Glaciology*, 53: 181–188.

Hewitt, K., 2011: Glacier change, concentration, and elevation effects in the Karakoram Himalaya, upper Indus basin. *Mountain Research and Development,* 31(3): 188–200.

Holzer, N., Vijay, S., Yao, T., Xu, B., Buchroithner, M., and Bolch, T., 2015: Four decades of glacier variations at Muztag Ata (eastern Pamir): a multi-sensor study including Hexagon KH-9 and Pleiades data. *The Cryosphere*, 9: 2071–2088.

Holzer, N., Golletz, T., Buchroithner, M., and Bolch, T., 2016: Glacier variations in the Trans Alai Massif and the Lake Karakul catchment (northeastern Pamir) measured from space. *In* Singh, R. B., Schickhoff, U., and Mal, S. (eds.), *Climate Change, Glacier Response, and Vegetation Dynamics in the Himalaya*. Switzerland: Springer, 139–153.

Jamieson, S. S. R., Ewertowski, M. W., and Evans, D. J. A., 2015: Rapid advance of two mountain glaciers in response to mine-related debris loading, *Journal of Geophysical Research Earth Surface*, 120: 1418–1435.

Jiskoot, H., 2011: Glacier surging. *In* Singh, V. P., Singh, P., and Haritashya, U. K. (eds.), *Encyclopedia of Snow, Ice and Glaciers.* Encyclopedia of Earth Sciences Series. Dordrecht: Springer, 415–428.

Jiskoot, H., Boyle, P., and Murray, T., 1998: The incidence of glacier surging in Svalbard: evidence from multivariate statistics. *Computers and Geosciences,* 24(4): 387–399.

Jiskoot, H., Murray, T., and Boyle, P., 2000: Controls on the distribution of surge-type glaciers in Svalbard. *Journal of Glaciology*, 46(154): 412–422.

Kamb, B., 1987: Glacier surge mechanism based on linked cavity configuration of the basal water conduit system. *Journal of Geophysical Research,* 92 (89): 9083–9100.

Koppes, M., Gillespie, A. R., Burke, R. M., Thompson, S. C., and Stone, J., 2008: Late Quaternary glaciation in the Kyrgyz Tien Shan. *Quaternary Science Reviews,* 27: 846–866.

Kotlyakov, V. M., 2004: Natural disasters in Russia. *In* Stoltman, J. P., Lidstone, J., and DeChano, L. M. (eds.), *International Perspectives on Natural Disasters: Occurrence, Mitigation, and Consequences.* Dordrecht: Kluwer Academic Publishers, 247–262.

Kotlyakov, V., Osipova, G., and Tsvetkov, D. G., 2008: Monitoring surging glaciers of the Pamirs, Central Asia, from space. *Annals of Glaciology,* 48: 125–134.

Kotlyakov, V. M., Dyakova, A. M., Koryakin, V. S., Kravtsova, V. I., Osipova, G. B., Varnakova, G. M., Vinogradov, V. N., Vinogradov, O. N., and Zverkova, N. M., 2010: Glaciers of the former Soviet Union. *In* Williams, R. S., Jr., and Ferrigno, J. G., (eds.), *Satellite Image Atlas of Glaciers of the World*. U.S. Geological Survey Professional Paper 1386-F-1, 125 pp.

Kutuzov, S., and Shahgedanova, M., 2009: Glacier retreat and climatic variability in the eastern Terskey-Alatoo, inner Tien Shan between the middle of the 19th century and beginning of the 21st century. *Global and Planetary Change,* 69: 59–70.

Lingle, C. S., and Fatland, D. R., 2003: Does englacial water storage drive temperate glacier surges? *Annals of Glaciology*, 36(1): 14–20.

Makarevich, K., 1952: Issledovaniye lednika Shokal'skogo v Zailiyskom Alatau v 1951 g. (Studies of Shokalskiy glaciers in Zailiyskiy Alatau in 1951). Moscow Editon "Mysl": Collected articles: Conquered peaks, 308–333 (in Russian).

Makarevich, K. G., and Fedulov, I. Ya., 1974: Pul'satsii lednika Shokalskogo v Zailiyskom Alatau (Surges of the Shokalsky glacier in Zailiysky Alatau). *Data of Glaciological Studies,* 24: 96–101 (in Russian).

Mavlyudov, B. R., 1995: Kolebanja jasyka lednika Severnyj Inylchek (Tongue oscillations of Northern Inylchek Glacier). *Data of Glaciological Studies,* 79: 95–98 (in Russian).

Mavlyudov, B. R., 1999: Lednik Inylchek I osero Mertzbachera. Sostojanne v 1997 godu (Lednik Inylchek and Lake Mertzbacher. Status of the year 1997). *Data of Glaciological Studies,* 86: 144–148 (in Russian).

Mayer, C., Fowler, A. C., Lambrecht, A., and Scharrer, K., 2011: A surge of North Gasherbrum, Karakoram, China. *Journal of Glaciology,* 57(205): 904–916.

Meier, M. F., and Post, A. S., 1969: What are glacier surges? *Canadian Journal of Earth Sciences*, 6(4): 807–817.

Murray, T., Stuart, G. W., Miller, P. J., Woodward, J., Smith, A. M., Porter, P. R., and Jiskoot, H., 2000: Glacier surge propagation by thermal evolution at the bed. *Journal of Geophysical Research,* 105(B6): 13491–13507.

Narama, C., Kääb, A., Duishonakunov, M., and Abdrakhmatov, K., 2010: Spatial variability of recent glacier area changes in the Tien Shan Mountains, Central Asia, using Corona (1970), Landsat (2000), and ALOS (2007) satellite data, *Global and Planetary Change*, 71(1-2): 42–54.

Nuth, C., and Kääb, A., 2011: Co-registration and bias corrections of satellite elevation data sets for quantifying glacier thickness change. *The Cryosphere*, 5: 271–290.

Osipova, G., and Khromova, T., 2010: Elektronnaja baza dannykh "Pulsiruyuchne ledniki Pamira" (Electonic data base "Suring glaciers of Pamir"). *Ice and Snow*, 4: 15–24.

Osmonov, A., 1968: Lednik Mushketova (Mushketov glacier). *Proceedings of the Kyrgyz SSR Geographical Society*, 7: 24–29 (in Russian).

Osmonov, A., 1974: *Sovremennoe oledenenie vostochnoy chasti bassena reki Sary-Jaz*. (*The Modern Glaciations of the Eastern Part of the Sary-Jaz River Basin)*. PhD thesis, Kirgiz State University, Frunze, 161 pp. (in Russian).

Osmonov, A., Bolch, T., Xi. C., Kurban, A., and Guo, W., 2013: Glaciers characteristics and changes in the Sary-Jaz River Basin (Central Tien Shan) 1990–2010. *Remote Sensing Letters,* 4(8): 725–734.

Paul, F., 2015: Revealing glacier flow and surge dynamics from animated image sequences: examples from the Karakoram. *The Cryosphere,* 9: 2201–2214.

Paul, F., Barrand, N., Berthier, E., Bolch, T., Casey, K., Frey, H., Joshi, S. P., Konovalov, V., Le Bris, R., Mölg, N., Nosenko, G., Nuth, C., Pope, A., Racoviteanu, A., Rastner, P., Raup, B., Scharrer, K., Steffen, S., and Winsvold, S., 2013: On the accuracy of glacier outlines derived from remote sensing data. *Annals of Glaciology,* 54(63): 171–182.

Pfeffer, W. T., Arendt, A. A., Bliss, A., Bolch, T., Cogley, J. G., Gardner, A. S., Hagen, J. O., Hock, R., Kaser, G., Kienholz, C., Miles, E. S., Moholdt, G., Mölg, N., Paul, F., Radić, V., Rastner, P., Raup, B. H., Rich, J., Sharp, M. J., and the Randolph Consortium, 2014: The Randolph Glacier Inventory: a globally complete inventory of glaciers. *Journal of Glaciology*, 60(221): 537–551.

Pieczonka, T., and Bolch, T., 2015: Region-wide glacier mass budgets and area changes for the Central Tien Shan between ~1975 and 1999 using Hexagon KH-9 imagery. *Global and Planetary Change,* 128: 1–13.

Pieczonka, T., Bolch, T., Junfeng, W., and Shiyin, L., 2013: Heterogeneous mass loss of glaciers in the Aksu-Tarim Catchment (Central Tien Shan) revealed by 1976 KH-9 Hexagon and SPOT-5 stereo imagery. *Remote Sensing of Environment,* 130: 233–244.

Post, A., 1969: Distribution of surging glaciers in western North America. *Journal of Glaciology*, 8(53): 229–240.

Quincey, D. J., and Luckman, A., 2014: Brief communication. On the magnitude and frequency of Khudropin glacier surge events. *The Cryosphere,* 8: 571–574.

Quincey, D. J., Glasser, N. F., Cook, S. J., and Luckman, A., 2015: Heterogeneity in Karakoram glacier surges. *Journal of Geophysical Research: Earth Surface*, 120: 1288–1300.

Raup, B., Racoviteanu, A., Khalsa, S. J. S., Helm, C., Armstrong, R., and Arnaud, Y., 2007: The GLIMS Geospatial Glacier Database: a new tool for studying glacier change, *Global and Planetary Change*, 56: 101–110.

Sevestre, H., and Benn, D. I., 2015: Climatic and geometric controls on the global distribution of surge-type glaciers: implications for a unifying model of surging. *Journal of Glaciology,* 61(228): 646–662.

Shangguan, D. H., Bolch, T., Ding, Y. J., Kröhnert, M., Pieczonka, T., Wetzel, H. U., and Liu, S. Y., 2015: Mass changes of Southern and Northern Inylchek Glacier, Central Tien Shan. *The Cryosphere,* 9: 703–717.

Solomina, O. N., Barry, R., and Bodnya, M., 2004: The retreat of Tien Shan glaciers (Kyrgyzstan) since the Little Ice Age. *Geografiska Annaler, Series A, Physical Geography,* 86(2): 205–215.

Sorg, A., Bolch, T., Stoffel, M., Solomina, O., and Beniston, M., 2012: Climate change impact on glaciers and runoff in Tien Shan (Central Asia). *Nature Climate Change,* 2: 725–731.

Surazakov, A. B., and Aizen, B. V., 2010: Positional accuracy evaluation of declassified Hexagon KH-9 mapping camera imagery. *Photogrammetric Engineering and Remote Sensing,* 76(5): 603–608.

Unger-Shayesteh, K., Vorogushyn, S., Farinotti, D., Gafurov, A., Deuthmann, D., Mandychev, A., and Merz, B., 2013: What do we know about past changes in the water cycle of Central Asia headwaters? A review. *Global and Planetary Change,* 110: 4–25.

Vilesov, E. N., and Khonin, R. V., 1967: Katalog Lednikov SSSR, Tsentralnyj i Yuzhnyj Kazakhstan, vol. 13. Leningrad (in Russian).

Watson, D., 1992: *Contouring: a Guide to the Analysis and Display of Spatial Data*. Tarrytown, New York: Elsevier Science.

Willis, I. C., 1995: Intra-annual variations in glacier motion: a review. *Progress in Physical Geography,* 19(1): 61–106.

Zabirov, R. D., 1961: About the state of some Tien Shan glaciers during the period of the International Geophysical Year (IGY). *IAHS Publication,* 54: 405–411.

MS submitted 14 March 2016
MS accepted 15 December 2016

APPENDIX

TABLE A1

Satellite data utilized for the study.

Sl No.	Sensor	Date*	Spatial resolution (m)	Usage	Mapping uncertainty (m)
1	KH-4A Corona	27/11/1964	2.7	Glacier Mapping + Mass budget	5.4
2	KH-4A Corona	08/08/1967	2.7	Glacier Mapping	5.4
3	KH-4 Corona	15/12/1962	7.6	Glacier Mapping	15.2
4	KH-2 Corona	07/12/1960	9.1	Glacier Mapping	18.2
5	KH-4A Corona	27/09/1968	2.7	Glacier Mapping	5.4
	KH-4B Corona	17/09/1971	1.8	Glacier Mapping	3.6
6	KH-9 Hexagon	31/07/1973	7.6	Glacier Mapping + Mass budget	15.2
7	KH-9 Hexagon	21/08/1980	7.6	Glacier Mapping + Mass budget	15.2
8	KH-9 Hexagon	12/01/1976	7.6	Glacier Mapping + Mass budget	15.2
9	KH-9 Hexagon	16/11/1974	7.6	Glacier Mapping + Mass budget	15.2
10	Landsat MSS	07/09/1972	60	Glacier Mapping	30
11	Landsat MSS	04/10/1975	60	Glacier Mapping	30
12	Landsat MSS	13/08/1975	60	Glacier Mapping	30
13	Landsat MSS	14/08/1975	60	Glacier Mapping	30
14	Landsat MSS	23/09/1977	60	Glacier Mapping	30
15	Landsat MSS	16/08/1978	60	Glacier Mapping	30
16	Landsat TM	22/08/1989	30	Glacier Mapping	15
17	Landsat TM	06/06/1990	30	Glacier Mapping	15
18	Landsat TM	07/08/1990	30	Glacier Mapping	15
19	Landsat TM	13/07/1992	30	Glacier Mapping	15
20	Landsat TM	25/09/1993	30	Glacier Mapping	15
21	Landsat TM	03/09/1994	30	Glacier Mapping	15
22	Landsat TM	10/10/1996	30	Glacier Mapping	15
23	Landsat TM	22/08/1998	30	Glacier Mapping	15
24	Landsat TM	02/10/1998	30	Glacier Mapping	15
25	Landsat TM	06/09/2006	30	Glacier Mapping	15
26	Landsat TM	08/10/2006	30	Glacier Mapping	15
27	Landsat TM	30/07/2007	30	Glacier Mapping	15
28	Landsat TM	08/08/2007	30	Glacier Mapping	15
29	Landsat TM	16/10/2009	30	Glacier Mapping	15
30	Landsat TM	03/10/2010	30	Glacier Mapping	15
31	Landsat TM	19/08/2011	30	Glacier Mapping	15
32	Landsat TM	11/09/2011	30	Glacier Mapping	15
33	Landsat 7 ETM+SLC on	13/09/2000	15/30	Glacier Mapping	7.5/15
34	Landsat 7 ETM+SLC on	27/09/2000	15/30	Glacier Mapping	7.5/15
35	Landsat 7 ETM+SLC on	31/10/2000	15/30	Glacier Mapping	7.5/15
36	Landsat 7 ETM+SLC on	03/10/2002	15/30	Glacier Mapping	7.5/15
37	Landsat 7 ETM+SLC on	05/10/2002	15/30	Glacier Mapping	7.5/15
38	Landsat 7 ETM+SLC off	18/07/2003	15/30	Glacier Mapping	7.5/15

TABLE A1

(Continued)

Sl No.	Sensor	Date*	Spatial resolution (m)	Usage	Mapping uncertainty (m)
39	Landsat 7 ETM+SLC off	20/07/2003	15/30	Glacier Mapping	7.5/15
40	Landsat 7 ETM+SLC off	12/08/2003	15/30	Glacier Mapping	7.5/15
41	Landsat 7 ETM+SLC off	27/08/2006	15/30	Glacier Mapping	7.5/15
42	Landsat 7 ETM+SLC off	15/09/2007	15/30	Glacier Mapping	7.5/15
43	Landsat 7 ETM+SLC off	07/09/2010	15/30	Glacier Mapping	7.5/15
44	Landsat 7 ETM+SLC off	08/07/2011	15/30	Glacier Mapping	7.5/15
45	Landsat 7 ETM+SLC off	24/07/2011	15/30	Glacier Mapping	7.5/15
46	Landsat 7 ETM+SLC off	11/08/2012	15/30	Glacier Mapping	7.5/15
47	Landsat 7 ETM+SLC off	27/08/2012	15/30	Glacier Mapping	7.5/15
48	Landsat 7 ETM+SLC off	29/07/2013	15/30	Glacier Mapping	7.5/15
49	Landsat 7 ETM+SLC off	16/07/2014	15/30	Glacier Mapping	7.5/15
50	Landsat 8	31/08/2013	15/30	Glacier Mapping	7.5/15
51	Landsat 8	23/09/2013	15/30	Glacier Mapping	7.5/15
52	Landsat 8	25/09/2013	15/30	Glacier Mapping	7.5/15
53	Landsat 8	01/07/2014	15/30	Glacier Mapping	7.5/15
54	Landsat 8	09/08/2014	15/30	Glacier Mapping	7.5/15
55	Landsat 8	14/10/2014	15/30	Glacier Mapping	7.5/15
56	SPOT-3	25/11/1995	10	Glacier Mapping	20
57	SPOT-3	12/09/1996	10	Glacier Mapping	20
58	SPOT-3	07/10/1996	10	Glacier Mapping	20
59	SPOT-5	24/08/2007	2.5	Glacier Mapping	2.5
60	SPOT-5	18/09/2007	2.5	Glacier Mapping	2.5
61	SPOT-5	19/09/2007	2.5	Glacier Mapping	2.5
62	SPOT-5	01/02/2008	2.5	Glacier Mapping	2.5
63	SPOT-5	30/07/2009	2.5	Glacier Mapping	2.5
64	SPOT-5	02/11/2009	2.5	Glacier Mapping	2.5
65	SPOT-5	04/09/2010	2.5	Glacier Mapping	2.5
66	Cartosat-1	27/08/2006	2.5	Glacier Mapping + Mass budget	2.5
67	IRS-1C LISS III	27/09/1997	23.5	Glacier Mapping	23.5

*Dates given in dd/mm/yyyy.

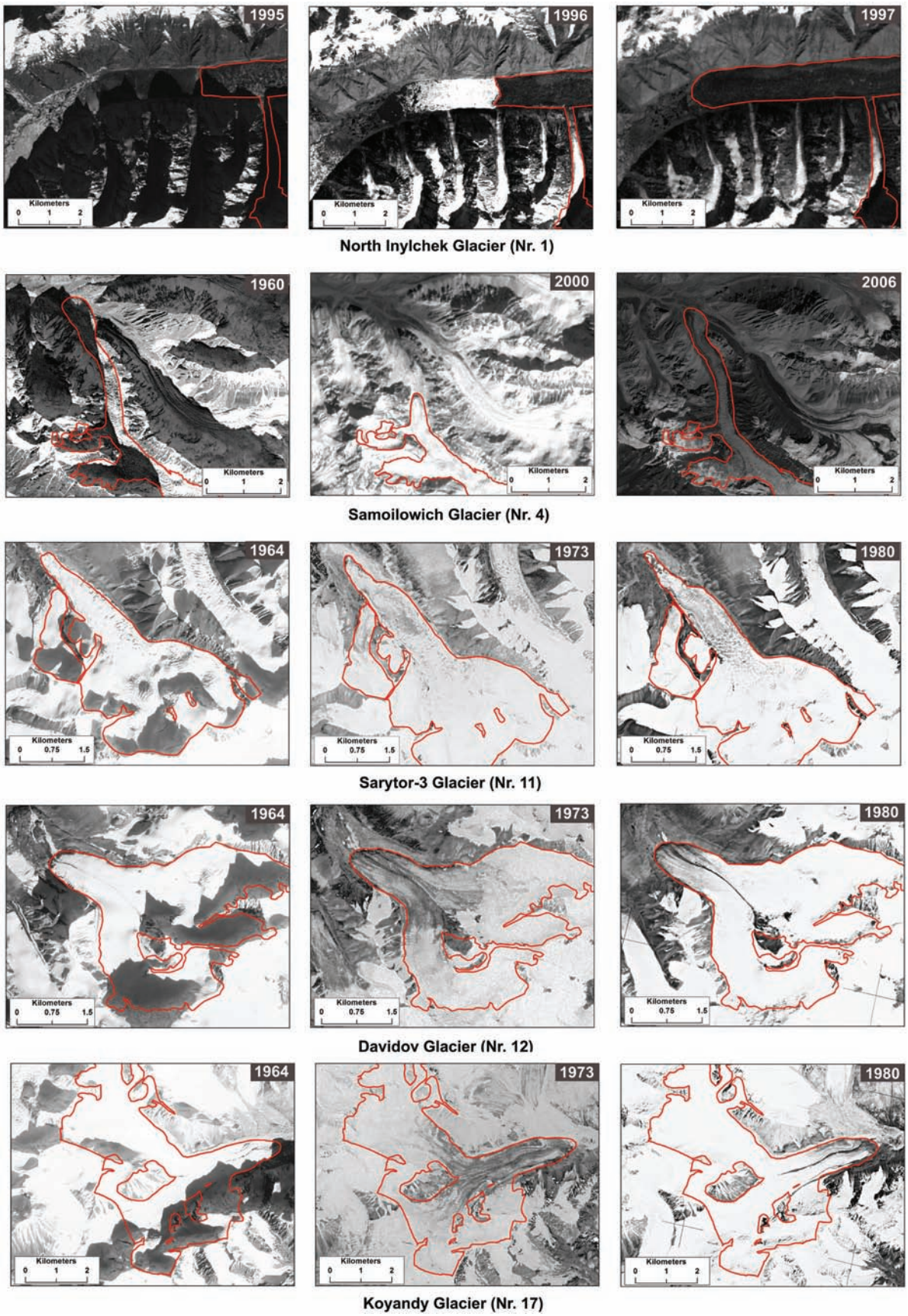

FIGURE A1. Surge in some glaciers of central Tien Shan and Ak-Shiirak.